

An Optimized Protein Kinase C Activating Diacylglycerol Combining High Binding Affinity (K_i) with Reduced Lipophilicity (log P)

Kassoum Nacro,^{†,‡} Dina M. Sigano,[‡] Shunqi Yan,[‡] Marc C. Nicklaus,[‡] Larry L. Pearce,[§] Nancy E. Lewin,[§] Susan H. Garfield,[#] Peter M. Blumberg,[§] and Victor E. Marquez^{*,‡}

Laboratory of Medicinal Chemistry, Center for Cancer Research, National Cancer Institute at Frederick, Frederick, Maryland 21702, and Laboratory of Cellular Carcinogenesis and Tumor Promotion and Laboratory of Experimental Carcinogenesis, Center for Cancer Research, National Cancer Institute, National Institutes of Health, Bethesda, Maryland 20892

Received January 31, 2001

A small, focused combinatorial library encompassing all possible permutations of acyl branched alkyl chains—small and large, saturated and unsaturated—was generated from the active diacylglycerol enantiomer (*S*-DAG) to help identify the analogue with the highest binding affinity (lowest K_i) for protein kinase C (PK-C) combined with the minimum lipophilicity (log P). The selected ligand (**3B**) activated PK-C more effectively than *sn*-1,2-diocanoylglycerol (diC8) despite being 1.4 log units more hydrophilic. Compound **3B** indeed represents the most potent, hydrophilic DAG ligand to date. With the help of a green fluorescent protein (GFP)-tagged PK-C α , **3B** was able to translocate the full length protein to the membrane with an optimal dose of 100 μ M in CHO-K1 cells, while diC8 failed to achieve translocation even at doses 3-fold higher. Molecular modeling of **3B** into an empty C1b domain of PK-C δ clearly showed the existence of a preferred binding orientation. In addition, molecular dynamic simulations suggest that binding discrimination could result from a favorable van der Waals (VDW) interaction between the large, branched *sn*-1 acyl group of **3B** and the aromatic rings of Trp252 (PK-C δ) or Tyr252 (PK-C α). The DAG analogue of **3B** in which the acyl groups are reversed (**2C**) showed a decrease in binding affinity reflecting the capacity of PK-C to effectively discriminate between alternative orientations of the acyl chains.

Introduction and Background

Protein kinase C (PK-C) is a family of serine/threonine-specific isozymes that are regulated by phosphorylation, by calcium, and by association with phospholipids and 1,2-diacylglycerol (DAG).^{1–4} Typically, these isozymes are cytosolic in the inactive state and, as part of the activation process, translocate to the inner leaflet of the cellular membrane.^{5,6} Classical (α , β , and γ) as well as novel (δ , ϵ , η , and θ) PK-C isozymes become activated as a result of the association of the cytosolic enzyme with membranes containing acid phospholipids.^{7,8} This association is strongly facilitated by the lipophilic second messenger, DAG, which is generated as a result of a stimulus-initiated activation of phospholipase C.⁹ The binding of PK-C to the plasma membrane is transient and regulated by its association with DAG in the membrane.¹⁰

DAG binds to the C1 domain of both the classical and novel members of the PK-C family to activate their downstream pathways.¹¹ Modeling experiments using the crystal coordinates of the C1b domain of PK-C δ in complex with phorbol-13-O-acetate¹² revealed two pos-

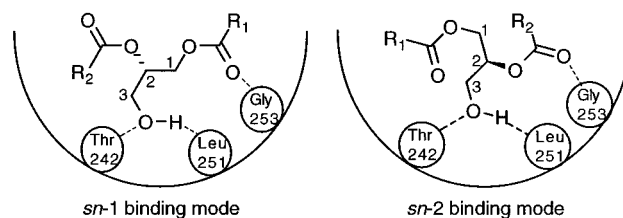


Figure 1. Hydrogen bonding interaction of DAG at the C1 domain of PK-C δ in the alternative binding modes of *sn*-1 and *sn*-2. Numbering of the DAG carbon backbone is shown.

sible binding orientations when DAG was docked into the empty C1b domain. These two apparently comparable binding modes, *sn*-1 and *sn*-2, form an identical network of hydrogen bonds with amino acids Thr242, Leu251, and Gly253, as was observed with phorbol-13-O-acetate in the crystal structure of the complex, and are shown schematically in Figure 1. Based on the two nonequivalent carbonyl moieties of DAG, the *sn*-1 binding mode is defined as that in which the *sn*-1 carbonyl and the hydroxyl group form hydrogen bonds to the protein. In the alternative *sn*-2 binding mode, the *sn*-2 carbonyl and the hydroxyl group are engaged in hydrogen bonding to the protein. A prediction is that these two binding orientations can direct the hydrophobic groups (R_1 and R_2) of the ligand in rather different directions and that differences in binding affinities should reflect preferences between these two binding modes (Figure 1). Consistent with this prediction, we sought to discriminate between these two binding alternatives by using an array of different alkyl chains

* Corresponding author. Phone: 301-846-5954. Fax: 301-846-6033. E-mail: marquezv@mail.nih.gov.

[†] Present address: Research Bldg., Suite W224A, Lombardi Cancer Center, Georgetown University, 3970 Reservoir Rd., NW, Washington, DC 20007.

[‡] National Cancer Institute at Frederick.

[§] Laboratory of Cellular Carcinogenesis and Tumor Promotion, National Institutes of Health.

[#] Laboratory of Experimental Carcinogenesis, National Institutes of Health.

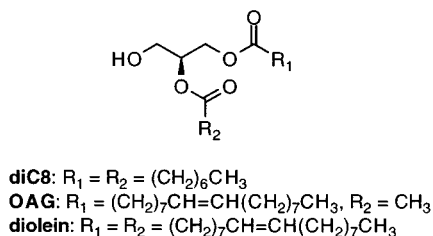


Figure 2. Common commercially available DAGs.

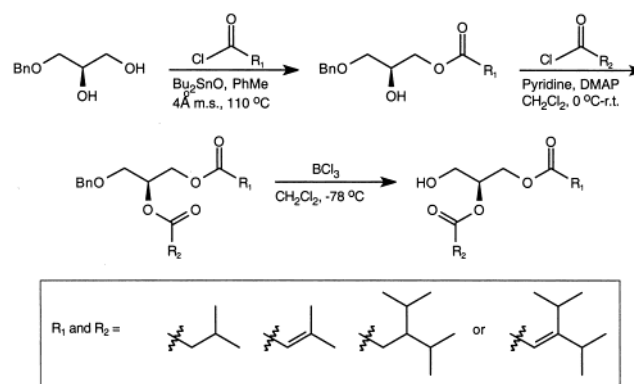
on DAG. An additional objective was also to select from this array a DAG ligand with adequate solubility (low lipophilicity) suitable for crystallographic and NMR studies with the C1b domain of PK-C δ . Finally, the biological activity of the selected ligand was to be compared to that of a prototypic DAG in terms of PK-C activation and ability to translocate the enzyme from the cytosol to the membrane.

It is well-known that the phorbol esters function as potent and metabolically stable DAG surrogates. In fact, the phorbol esters bind to PK-C with affinities that are several orders of magnitude greater than those of the commonly studied DAGs.¹³ Among the most commonly used DAGs in PK-C studies are the commercially available 1,2-dioctanoyl-*sn*-glycerol (diC8), 1-oleoyl-2-acetyl-*sn*-glycerol (OAG), and 1,2-dioleoyl-*sn*-glycerol (diolein) (Figure 2).

Over the past few years, we have attempted to bridge the affinity gap between phorbol esters and DAGs by two independent approaches. One approach includes reducing the entropic penalty associated with DAG binding by constraining the glycerol backbone into DAG-lactones.¹⁴ A second approach includes increasing the bulk of the acyl groups by incorporating highly branched alkyl chains capable of interacting more efficiently with a group of conserved amino acids in the space between the two β sheets of the C1b domain.^{14–16} Since branched alkyl chains are less lipophilic than their linear counterparts, we have decided to reduce the lipophilicity (log P) of DAG further to levels that would allow the detection of differences between the *sn*-1 and *sn*-2 binding modes by combining small and large, branched alkyl chains.

While the role of the alkyl chain in DAGs has been principally correlated with providing adequate lipophilicity to facilitate partitioning into a lipid-rich environment, the docking of DAG into the C1b domain of PK-C δ —as in the case of the DAG-lactones—revealed potentially important hydrophobic contacts with the protein which could extend into the protein-membrane interface (vide infra). Thus, any increase in binding affinity due to the branched alkyl chains in DAG would probably result from a combination of two factors: adequate membrane partitioning and hydrophobic contacts with the protein. We anticipated that by reducing the lipid dependency required for membrane distribution to an absolute minimum, the compounds would be more effectively discriminated by the protein in terms of the two possible binding modes (*sn*-1 versus *sn*-2). For that reason, we designed a small combinatorial library based on a uniform "core" *S*-DAG enantiomer with variable R_1 and R_2 groups containing branched alkyl chains, small and large, saturated and unsaturated (Scheme 1, Table 1).

Scheme 1



Since the calculated lipophilicities for PDBU (phorbol-12,13-O-dibutyrate) and prostratin (12-deoxyphorbol-13-O-acetate) expressed as log P values (see Table 2) are lower than that of the least lipophilic, commercially available DAG (diC8), we undertook the task of identifying a DAG candidate where a decrease in the log P value would not compromise binding affinity. Hence, by reducing lipophilicity, nonspecific binding interactions between DAG and the membrane would be minimized, and differences in K_i values would be expected to reflect changes in specific interactions with the protein.

Results and Discussion

Synthesis. A small combinatorial library of 16 DAGs was prepared to help identify the optimal DAG for PK-C combining the highest binding affinity with the lowest log P value. In selecting the R_1 and R_2 alkyl groups, consideration was also given to the possibility of reducing the entropy of binding by restricting the rotation about the α,β -bond of the alkyl chain. Thus, analogous alkyl chains were designed in which the α,β σ -bond was replaced with a π -bond to analyze its effect on binding affinity (see Scheme 1).

The target compounds were synthesized in three simple steps starting from commercially available (R)-(+)-3-benzyloxy-1,2-propanediol (Scheme 1). Monoacylation at the *sn*-1 position was followed by a second acylation step at the *sn*-2 position, and debenzoylation gave the asymmetrically substituted target compounds. In cases where the acyl groups at both the *sn*-1 and *sn*-2 positions were the same, the target compounds were easily synthesized in just two steps. Hence, by using 2 equiv of the activated acid, both the *sn*-1 and *sn*-2 positions could be acylated in the same reaction. Debenzylation then gave the symmetrically substituted target compounds.

Biological Activity. The interaction of all of DAGs with PK-C was assessed in terms of the ability of the ligand to displace bound [20-³H]phorbol-12,13-dibutyrate (PDBU) from a recombinant single isozyme (PKC- α) in the presence of phosphatidylserine. The inhibition curves obtained for all ligands were of the type expected for competitive inhibition, and the ID₅₀ values were determined by fit of the data points to the theoretical noncooperative competition curve. The K_i 's for inhibition of binding (Table 1) were calculated from the ID₅₀ values. The octanol/water partition coefficients (log P) were calculated according to the fragment-based program KOWWIN 1.63.¹⁷

Table 1. Small Combinatorial DAG Library with Log P and K_i Value (in nM)

I		II	
	1A log P = 2.16 $K_i = 1409 \pm 94$		1C log P = 3.97 $K_i = 74.9 \pm 7.2$
	1B log P = 2.07 $K_i = 1050 \pm 240$		1D log P = 3.89 $K_i = 330 \pm 22$
	2A log P = 2.07 $K_i = 1800 \pm 110$		2C log P = 3.88 $K_i = 154 \pm 15$
	2B log P = 1.99 $K_i = 2400 \pm 160$		2D log P = 3.80 $K_i = 68.3 \pm 7.3$
	3A log P = 3.97 $K_i = 71 \pm 12$		3C log P = 5.79 $K_i = 28.6 \pm 3.2$
	3B log P = 3.88 $K_i = 39.9 \pm 1.9$		3D log P = 5.71 $K_i = 31.1 \pm 2.1$
	4A log P = 3.89 $K_i = 110 \pm 12$		4C log P = 5.71 $K_i = 24.6 \pm 1.7$
	4B log P = 3.80 $K_i = 73 \pm 10$		4D log P = 5.62 $K_i = 44.5 \pm 4.6$
III		IV	

Table 2. Commonly Used DAGs and Phorbol Esters with Log P and K_i Value.

compound	log P ^a	$K_i \pm \text{SEM}$ (nM) ^b
diolein (1,2-dioleoyl- <i>sn</i> -glycerol)	14.6	87.2 ± 1.6
OAG (1-oleoyl-2-acetate- <i>sn</i> -glycerol)	7.0	50.4 ± 4.2
diC8 (<i>sn</i> -1,2-dioctanoylglycerol)	5.3	33.0 ± 1.46
PDBu (phorbol-12,13-dibutyrate)	3.4	0.2 ± 0.03
prostratin	1.9	4.8 ± 0.4^{25}

^a Octanol/water partition coefficients (log P).¹⁷ ^b Values represent the mean \pm standard error (triplicate).

All of the possible combinations using large and small, saturated and unsaturated, branched alkyl chains are represented in Table 1 and can be visualized in four quadrants. The *sn*-1 substituent remains constant across the rows, while the *sn*-2 substituent remains constant down the columns.

The compounds in quadrant I (**1A**, **1B**, **2A**, and **2B**) are all substituted with the smaller isopropyl and isopropenyl chains. These compounds contain similar size branched alkyl groups, and all combinations of saturated and unsaturated chains are shown. The K_i values of these compounds are in the micromolar range and log P values are around 2. The poor binding affinity shown by the compounds in quadrant I can be attributed to a lack of adequate lipophilicity due to the small isopropyl/isopropenyl groups. These groups may be too small to meet a minimum required lipophilic threshold and hence cannot properly partition the DAG into the membrane.

On the other extreme, the compounds in quadrant IV (**3C**, **3D**, **4C**, and **4D**) are all substituted with the larger and equally bulky diisopropylethyl and diisopropylethenyl, branched alkyl chains. All combinations of

saturated and unsaturated chains are represented. The more efficient binding reflected by the smaller K_i values (compared to the compounds in quadrant I) can be attributed to the increased lipophilicity ($\log P = \text{ca. } 5.7$ versus $\text{ca. } 2$) associated with the larger alkyl groups. Thus, these compounds appear to have significant hydrophobicity to properly concentrate at the membrane and are able to bind to the protein with comparable high binding affinities. The $\log P$ and K_i values closely match the corresponding values for diC8 (see Table 2). These results appear to indicate that when the branched alkyl chains are of similar size, as they are within quadrants I and IV, there is little or no discrimination in binding mode preference. Perhaps this can be ascribed to the inability of the PK-C:membrane complex to distinguish between *sn*-1 and *sn*-2 alkyl groups of similar size. Thus, there would not be a strong preference for one binding mode over the other if DAG chooses a preferred binding mode based on the nature of its alkyl groups.

When the *sn*-1 and *sn*-2 positions are unsymmetrically substituted and therefore *not* of the same size, as shown within quadrants II and III, *and* the compounds contain fully saturated, or completely unsaturated alkyl chains (**1C**, **2D**, **3A**, and **4B**), the absolute position (*sn*-1 versus *sn*-2) of the larger and smaller branched alkyl groups does not seem to have a significant effect either. However, when one of the unsymmetrical alkyl chains is unsaturated at either the *sn*-1 or *sn*-2 positions, the level of discrimination is quite significant as demonstrated along the diagonal (**1D**, **2C**, **3B**, and **4A**). This can be attributed to a reduction in the degrees of freedom at either the *sn*-1 or *sn*-2 position induced by the double bond compared to its saturated counterpart. Such an effect, combined with the reduced lipophilicity of the compounds, enhances the level of discrimination, allowing the detection of preferential binding interactions between the ligand and the protein.

The increased efficiency of PK-C in discriminating between DAG analogues along the **1D**, **2C**, **3B**, **4A** diagonal could be attributed to either the ligand being optimized for one binding mode over the other (Figure 1) or to the ability of PK-C to discriminate between different alkyl chain orientations in a single, preferred binding mode. Compound **3B** represents the DAG with the most efficient binding affinity; indeed, its $\log P$ value was reduced 1.5 log units relative to diC8 ($\log P_{3B} = 3.8$ versus $\log P_{\text{diC8}} = 5.3$) without compromising binding affinity ($K_{i(3B)} = 39.9 \text{ nM} \pm 1.9$ versus $K_{i(\text{diC8})} = 33.0 \text{ nM} \pm 1.46$). In **3B** the *sn*-1 alkyl group is large, while the *sn*-2 alkyl group is small and conformationally restricted. The reversal of these groups, as in **2C**, results in a *ca.* 4-fold decrease in binding affinity reflecting a remarkable discriminating ability by PK-C. Computational docking and molecular dynamic simulations (vide infra) suggest that binding discrimination could result from a favorable van der Waals (VDW) interaction between the large, branched *sn*-1 acyl group of **3B** and the aromatic ring of Trp252 (PKC- δ) or Tyr252 (PKC- α).

Since the C1b domain of PK-C δ is used as a "general receptor" for modeling, while actual binding affinities are measured against the complete α isozyme, it is important to remember that the C1b domain (amino acids 242–253) among classical (α , β , and γ) and novel

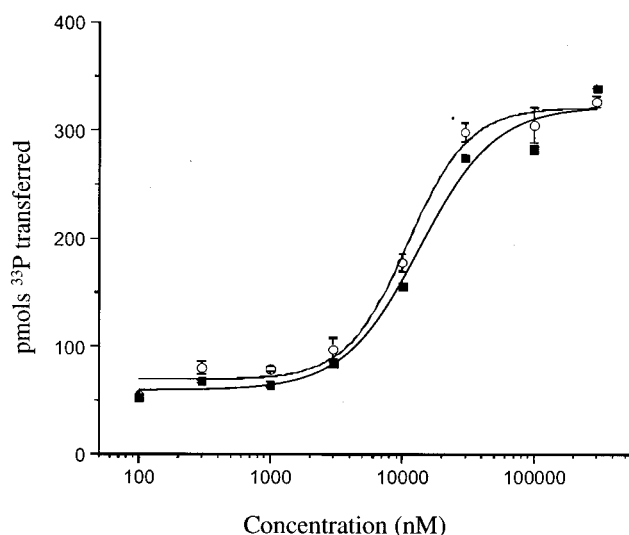


Figure 3. Stimulation of PK-C α kinase activity as a function of ligand concentration. Kinase activity of PK-C α was assayed in the presence of the indicated concentrations of **3B** (open circles) or diC8 (filled squares). Results are from a single experiment, with each point determined in triplicate. Two additional experiments gave similar results.

(δ , ϵ , η , and θ) PK-C isozymes is strictly conserved and that DAG has similar effects on all these isoforms. The only difference between the C1b domains of the α and δ isozymes is that Trp252 in PK-C δ is replaced by Tyr252 in PK-C α . The K_i value for **3B** against PK-C δ was in fact lower ($20.8 \text{ nM} \pm 1.8$), reflecting perhaps a more efficient VDW interaction between the branched *sn*-1 acyl group and the wider aromatic ring of Trp252.

Further evaluation of compound **3B** showed that it stimulated PK-C α enzymatic activity to a similar level as did diC8 (Figure 3). In addition, its half-maximally effective concentration for stimulation under these assay conditions was slightly less, reflecting better potency (**3B**, $9.5 \pm 0.8 \mu\text{M}$, $n = 3$; diC8, $16.4 \pm 2.9 \mu\text{M}$, $n = 3$). The values in parentheses represent mean \pm SEM for triplicate experiments. These results indicate that **3B** functions as an effective activator of PK-C.

In intact cells, phorbol esters and other activators of PK-C induce translocation from the cytosol to the membrane and other cellular compartments. This translocation can be visualized in the intact cells with fusion constructs between PK-C isoforms and a fluorescent tag, green fluorescent protein.¹⁸ Using green fluorescent protein (GFP)-tagged PK-C, the dynamics of PK-C translocation can be monitored in living cells and in real time. In Chinese hamster ovary (CHO-K1) cells transfected with PK-C α -GFP, **3B** induced translocation with an optimal dose of $100 \mu\text{M}$ (Figure 4); less extensive translocation was observed at $30 \mu\text{M}$; and variable, limited translocation was seen at $10 \mu\text{M}$ (data not shown). For comparison, diC8 at $300 \mu\text{M}$ induced no response, and translocation by 300 nM PDBu resembled that by $100 \mu\text{M}$ **3B**. These relative potencies for translocation generally agree with those obtained in the ligand binding assay. The difference between diC8 and **3B** is worth remarking since Oancea and Meyer have reported that while diC8 effectively translocated the GFP-tagged C1 domain of PK-C γ to the plasma membrane, it had no measurable effect on the full-length PK-C γ -GFP, even at doses 10-fold higher than those used

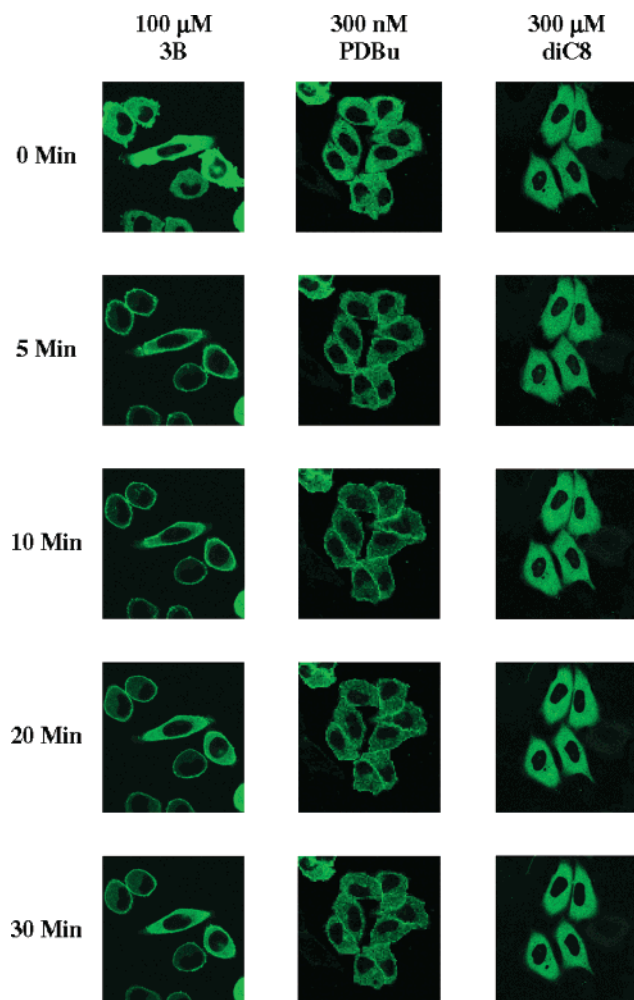


Figure 4. Translocation of PK-C α -GFP in response to **3B** and other ligands. PK-C α -GFP was expressed in CHO-K1 cells. Cells were treated as indicated with **3B**, with PDBu, or with diC8, and the localization of PK-C α -GFP was determined by confocal microscopy as a function of time. Images shown are of cells before treatment or after treatment for the times indicated. At least three experiments were performed and images shown are representative.

in this work.¹⁰ They explained their observation on the basis of the lower affinity of PK-C for DAG. However, despite the different PK-C isozyme involved, our results would suggest that this observation is only valid for diC8 since **3B** is a DAG analogue capable of translocating the full length PK-C α -GFP.

Computational Modeling

Autodock Study. Docking studies were performed using version 2.4 of AutoDock.¹⁹ The structure of the empty C1b domain of PK-C δ , grid setup, and parameters necessary for AutoDock and cluster analysis were the same as previously reported.¹⁵ Each ligand was subjected to 1000 steps of a Monte Carlo (MC) conformational search using the program Macromodel 7.0.²⁰ The minimum conformation reached by MC was then fully optimized at the semiempirical level using the AM1 Hamiltonian within the program InsightII,²¹ and the charges necessary for AutoDock were derived at this level. The docking simulation was repeated 100 times for each ligand starting with a randomly different conformation each time. The number of *sn*-1 and *sn*-2

Table 3. Percent of Docking Simulations in *sn*-1 and *sn*-2 Binding Modes⁵³

ligand	<i>sn</i> -1	<i>sn</i> -2	other
1A	42	6	52
1B	90	8	2
1C	45	45 ^a	10
1D	73	11 ^a	16
2A	82	12 ^a	6
2B	57	34 ^a	19
2C	49	38 ^a	23
2D	54	39 ^a	9
3A	89	1	10
3B	93	0	7
3C	63	20 ^a	17
3D	61	17 ^a	22
4A	83	8 ^a	9
4B	91	1	8
4C	56	32 ^a	12
4D	42	41 ^a	17

^a Very weak *sn*-2 binding with a distance between atoms involved in hydrogen bonding of 2.70–3.40 Å.

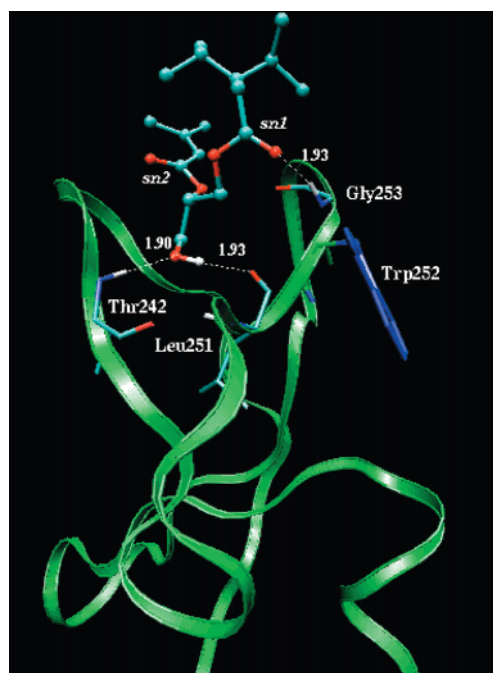


Figure 5. Docking results showing hydrogen-bonding interactions of **3B** with the C1b domain of PK-C δ in the *sn*-1 binding mode.

binding modes for each ligand are shown in Table 3. The results suggest that the *sn*-1 mode is preferred. In terms of the hydrogen-bonding network, the *sn*-2 binding mode appears weaker since most distances involved in hydrogen bonding were found to be greater than 2.70 Å. Figure 5 depicts the docking results obtained with **3B** displaying optimal hydrogen bond distances.

Flexible Docking. The *sn*-1 binding mode for the DAGs was also found to be energetically favorable by flexible docking with the Merck Molecular Force Field (MMFF) available in Macromodel.²⁰ The low-mode (LMOD) algorithm implemented in Macromodel was applied for the conformational search. Each ligand, together with six residues of the C1b domain (Ser240, Thr242, Leu251, Trp252, Gly253, and Leu254), was allowed to move freely during the simulation, while the rest of the residues were kept fixed. Each ligand was subjected to explicit translation/rotation in the binding site via the MOLS command in BatchMin. The simul-

Table 4. Electrostatic (elec), van der Waals (VDW), and Total Energies (kcal/mol) Calculated from MD Simulations for Ligands **2C**, **3B**, and **3C** in the Alternative *sn*-1 and *sn*-2 Binding Modes^a

		2C	3B	3C
total	<i>sn</i> -1	-38.12	-41.54	-41.63
	<i>sn</i> -2	-36.48	-34.83	-36.73
elec	<i>sn</i> -1	-13.14	-15.23	-15.62
	<i>sn</i> -2	-12.57	-12.72	-11.73
VDW	<i>sn</i> -1	-24.98	-26.25	-25.90
	<i>sn</i> -2	-23.92	-22.11	-25.00

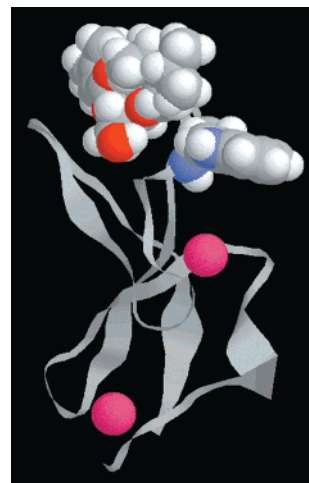
^a The simulations were performed at 298 K for 37–40 ns.

taneous translation and rotation of the ligand randomly varied between 0.1 and 0.5 Å and 0–90°, respectively. A 5000-step search was performed for the flexible docking of each of the 16 DAGs listed in Table 1. For DAGs **3B** and **2C**, a lengthy 25000-step search led to the same global minimum as the 5000-step search. For each ligand, more than 100 structures were found within a 30 kJ energy range, and in every case, more than 98% of the structures appeared with the ligand bound in the *sn*-1 binding mode at much lower energies than in the alternative *sn*-2 binding mode.

Molecular Dynamic Simulations. Molecular dynamics (MD) simulations of approximately 40 ns using the program CHARMM28A1²² were performed for **3B**, **2C**, and the symmetrically branched **3C** for both *sn*-1 and *sn*-2 binding modes inside the C1b domain of PK-C δ . The CHARMM force field, parametrized with the all-hydrogen PARAM27²³ parameter set, provided the potential energies. A dielectric constant of 2.0 was used to mimic the lipid environment of a transmembrane protein. No explicit water (solvent) molecules were added. The cutoff distance for nonbonded interactions was set to 14.0 Å. The cutoff distance at which the switching function eliminates all contributions from an interactive pair in calculating energies was set to 12.0 Å. A SHAKE algorithm was applied to constrain covalent bonds to hydrogens to 10⁻⁸ Å. Molecular dynamic simulations were carried out in parallel with 8 CPUs of an SGI Origin computer by heating for 80 ps and then equilibrating for 80 ps more at 298 K. A time step of 1 fs was used and the simulations were performed at 298 K for ca. 37–40 ns.

Zinc finger geometries ((Cys)₃–Zn–His) of PK-C were calculated at the Density Functional Theory (DFT) level using the B3LYP/6-311+G** basis set in Gaussian.²⁴ Ligands **3B** and **2C** were fully optimized with the level of B3LYP/6-31G* basis set in the gas phase, and the electrostatic potential-derived (ESP) charges were calculated from these geometries with either Jaguar 3.5 or 4.0 versions.²⁰ The corresponding parameters for zinc fingers and the ligands for MD simulations were derived from these optimized structures. The interaction energies between the protein and the ligand were calculated using the CHARMM command INTERACT. They are shown in Table 4 in kcal/mol.

For each representative ligand studied (**3B**, **2C**, and **3C**), the *sn*-1 binding mode appears to be energetically more favorable than the *sn*-2 binding mode. Even for the weakest ligand of this triad (**2C**), both electrostatic and VDW interactions favor the *sn*-1 binding mode. The same preference for the *sn*-1 mode was also observed for the better ligands, **3B** and **3C**, and the calculated energies in the *sn*-1 mode for the three ligands follow

**Figure 6.** Close approach between Trp252 and the branched *sn*-1 acyl chain of **3B** observed during MD simulation.

the order **3C** < **3B** < **2C**, which is in good agreement with the measured *K_i* values. The small energy difference between **3C** and **3B** correlates well with the similar experimentally measured *K_i* values (28.6 nM and 39.9 nM, respectively, Table 1). The lower *K_i* for **3C** relative to **3B** is probably the result of a more effective membrane partitioning due to the higher lipophilicity of the former; however, the nearly 100-fold difference in calculated lipophilicity ($\Delta \log P$ ca. 2) would not seem to be commensurate with the relative small difference in potency. In terms of an ideal relationship of *K_i* versus log *P*, **3B** remains the most potent DAG analogue. Ligand **3B** is also the most discriminating in terms of the binding energies for *sn*-1 versus *sn*-2 modes (compare **2C** versus **3B**, Table 4). Among other factors that could account for this phenomenon is a favorable VDW interaction between the large, branched *sn*-1 acyl chain and the flexible aromatic ring of Trp252 that was observed during the MD simulation with the C1b domain of PK-C δ (Figure 6). Relative to its position in the crystal structure (see Figure 5), Trp252 moves closer to the branched *sn*-1 acyl chain of **3B** to achieve a favorable hydrophobic contact during the MD simulation. As mentioned before, a similar favorable contact in the C1b domain of PK-C α could also occur between the branched *sn*-1 acyl chain of **3B** and Tyr252.

It is remarkable how all the structural factors must play a concerted role in determining affinity. Indeed, all the compounds in the same quadrant as **3B** have either a similar or equivalent branched acyl chain as **3B**, and yet they show weaker binding affinities. It is interesting to remark that according to the docking results (Table 3), compound **3B** has the highest percent of occupancy in the *sn*-1 binding mode. This means that a combination of factors, including hydrogen bonding, VDW interactions, and proper membrane partitioning, appears to have been optimized in **3B**.

Observations and Conclusions

By employing a combination of nonequivalent, large and small, branched alkyl chains as acyl groups of DAG, we have been able to decrease lipophilicity up to 1.5 log units lower than that of diC8 without sacrificing potency. However, a log *P* value lower than ca. 2 appears to be below the minimum lipophilic threshold required

for proper partitioning of DAG into the membrane. When both branched alkyl substituents are of the same size, there appears to be little discrimination in binding. On the other hand, when the alkyl chains are *not* of the same size *and* the compound is neither completely saturated nor unsaturated, the best combination is for the *sn*-1 substituent to be the larger, saturated branched alkyl group, and for the *sn*-2 substituent to be the smaller, unsaturated branched alkyl group.

From these studies we found compound **3B** to be the most potent DAG analogue in Table 1 with the lowest log *P* value. The combination of asymmetric alkyl branches and the specific location of the double bond in the small alkyl branch allow this molecule to discriminate effectively between two alternative binding modes while interacting with PK-C. Based on the overwhelming preference for the *sn*-1 binding mode demonstrated by three different modeling approaches, we conclude that DAGs prefer to bind in this modality and that the contrast between **3B** and its transposed analogue (**2C**) reflects the ability of PK-C to discriminate between different orientations of the two alkyl branches. Compound **2C** could also achieve the same disposition for the two alkyl branches as in **3B** but at the higher price of binding in the less favorable *sn*-2 binding mode. Therefore, when mixed binding modes are possible they are expected to produce lower binding affinities. We conclude that compound **3B** appears to have the structural attributes to overwhelmingly prefer the *sn*-1 binding mode (see Table 3).

Compound **3B** represents the most potent, hydrophilic DAG ligand to date. It activates PK-Cα ca. 2-fold better than diC8, and it is capable of translocating the full length protein efficiently to the membrane. This compound represents an ideal candidate for structural analysis in a complex with a C1 domain. The realization of this objective and a continuing comprehensive study of the biology of **3B** are issues of high priority in our laboratory.

Experimental Section

Analysis of Inhibition of [³H]PDBU Binding by Non-radioactive Ligands. Enzyme–ligand interactions were analyzed by competition with [³H]PDBU binding essentially as described previously with the single isozyme PK-Cα.¹⁵

Kinase Assay. Protein kinase C activity was assayed by measuring the incorporation of ³³P from [γ -³³P 3000 Ci/mmol] ATP (ICN, Costa Mesa, CA) into PK-Cα pseudosubstrate peptide [ser²⁵] PKC (Life Technologies, Rockville, MD) in the presence of PK-Cα, which was partially purified as described.²⁵ The assay buffer contained 20 mM Tris-C1 pH 7.5, 7.5 mM magnesium acetate, 0.1 mM CaCl₂, 0.25 mg/mL bovine serum albumin (fraction V) (Sigma, St. Louis, MO), 10 μg/mL phosphatidylserine, and 90 μg/mL phosphatidylcholine (Avanti Polar Lipids, Alabaster, AL) and activators phorbol 12-myristate,13-acetate (LC Laboratories, Woburn, MA), 1,2-dioctanoylglycerol (Avanti Polar Lipids, Alabaster, AL), or **3B**. The reaction was started with the addition of ATP (50 μM final concentration, 1 μCi) and 300 nM pseudosubstrate peptide and incubated at 30 °C for 10 min. The reaction was stopped by chilling on ice. A 25 μL aliquot was spotted onto DE81 ion exchange chromatography paper (Whatman Ltd., Maidstone, England). The paper was washed three times in 0.5% phosphoric acid. The bound radioactivity was measured in a scintillation counter. In each experiment, each ligand concentration was assayed in triplicate. The dose response curve was fitted to the relationship $y = [(A_1 - A_2)/(1 + (X/X_0)^p)] + A_2$, where

*A*₁ represents basal activity, *A*₂ represents maximal stimulated activity, *X* represents the concentration of activator, and *X*₀ represents the half-maximally effective dose.

Cell Culture. CHO-K1 cells (CCL 61) were obtained from the American Type Culture Collection (Manassas, VA). The cells were cultured at 37 °C in Dulbecco's modified Eagle's medium supplemented with 4500 mg/L glucose, 4 mM L-glutamine, and 10% fetal bovine serum (Life Technologies, Inc. Rockville, MD) in a humidified atmosphere containing 5% CO₂. The cells were subcultured twice a week and reseeded at 10⁶ cells/T-75 tissue culture flask.

Expression of PKCα-GFP Fusion Protein. The cDNA encoding bovine PK-Cα fused to a variant of green fluorescent protein (GFP) was constructed as reported for PK-Cδ GFP.²⁶ CHO-K1 cells were grown on 40 mm round coverslips (Bioprotechs, Inc., Butler, PA) at a seeding density of 2.5 × 10⁵ cells per dish. Transient transfection was conducted using LipofectAMINE PLUS (Life Technologies, Inc. Rockville, MD) according to the manufacturer's protocol. The fluorescence became detectable 24 h after transfection, and all experiments were performed 48 h after transfection. Before imaging of the cells, the medium was aspirated from the cells and replaced with DMEM plus 10% fetal bovine serum without phenol red (Life Technologies, Rockville, MD). All PK-C activators were diluted in the same medium with the final concentration of solvent (DMSO) always less than 0.1%. The cells were perfused up to 1 h with specified concentrations of the activators phorbol 12,13-dibutyrate (LC Services, Woburn, MO), 1,2-dioctanoylglycerol (Avanti Polar Lipids, Alabaster, AL), and **3B**.

Confocal Imaging. Confocal fluorescent images were collected with a Bio-Rad MRC 1024 confocal scan head (Bio-Rad, Hercules, CA) mounted on a Nikon Optiphot microscope with a ×60 planapochromat lens. Excitation at 488 nm was provided by a krypton–argon gas laser with a 522/32 emission filter for green fluorescence. For live cell imaging, a Biotech Focht Chamber System (Bioprotechs, Butler, PA) was inverted and attached to the microscope stage with a custom stage adapter. The cells plated on the 40-mm round coverslip were enclosed in the chamber and connected to a temperature controller set at 37 °C, and medium was perfused through the chamber with a Lambda microperfusion pump. Sequential images of the same cells were collected at one minute time points using LaserSharp software.

General Procedures. All chemical reagents were commercially available. Melting points were determined on a MelTemp II apparatus, Laboratory Devices, USA, and are uncorrected. Silica gel chromatography was performed on silica gel 60, 230–400 mesh (E. Merck). ¹H and ¹³C NMR spectra were recorded on a Bruker AC-250 instrument at 250 and 62.9 MHz, respectively. Spectra are referenced to the solvent in which they were run (7.24 ppm for CDCl₃). Infrared spectra were recorded on a Perkin-Elmer 1600 series FT-IR. Optical rotations were recorded on a Perkin-Elmer model 241 polarimeter at room temperature with a path length = 1 dm. Positive ion fast-atom bombardment mass spectra (FAB-MS) were obtained on a VG 7070E mass spectrometer at an accelerating voltage of 6 kV and a resolution of 2000. Glycerol was used as the sample matrix and ionization was effected by a beam of xenon atoms. Elemental analyses were performed by Atlantic Microlab, Inc., Atlanta, GA.

4-Methyl-3-(isopropyl)pent-2-enoyl Chloride. Under argon, oxalyl chloride (1.8 mL) and pyridine (52 μL) were added dropwise to a 0 °C solution of 4-methyl-3-(isopropyl)-pent-2-enoic acid (2.0 g) in Et₂O (26 mL). The solution was allowed to reach room temperature and stirred 44 h. The reaction mixture was then filtered through Celite, and the filtrate was concentrated to give the acid chloride as a thin pale yellow oil (2.03 g, 91%). This compound was used without further purification. IR (neat) 2963 (CH), 1774 (C=O), 1600 (C=C), 996 (CCl) cm⁻¹; ¹H NMR (250 MHz, C₆D₆) δ 0.66 and 0.73 (d, *J* = 6.8 Hz, 12 H, ClC(O)CH=C(CHMe₂)₂), 2.06 and 3.65 (heptet, *J* = 6.8 Hz, 2 H, ClC(O)CH=C(CHMe₂)₂), 5.92 (s, 1 H, ClC(O)CH=C(CHMe₂)₂); ¹³C NMR (62.5 MHz, C₆D₆) δ 19.39, 23.02, 29.55, 30.99, 119.66, 163.23, 182.36.

General Procedure for the Synthesis of 1-Substituted-3-benzyl Glycerols. Under argon, dibutyltin oxide (2.0 equiv) was added to a stirring solution of (R)-(+)-3-benzoyloxy-1,2-propanediol (1.0 equiv) in toluene (15 mL/mmol) containing 4 Å molecular sieves. The mixture was then heated to reflux for 3 h, after which it was cooled to 0 °C, and the acyl chloride (1.1 equiv) was added dropwise. The ice bath was removed, and the reaction was stirred for 90 min. The reaction was quenched with pH 7 buffer solution and diluted with CHCl_3 . The mixture was washed with brine, extracted twice with CHCl_3 , dried over MgSO_4 , and concentrated. Purification by silica gel column chromatography (2:1 hexane:ether) gives the named product as a colorless oil.

1-(3-Methylbutanoyl)-3-benzyl-*sn*-glycerol. (R)-(+)-3-benzoyloxy-1,2-propanediol and 3-methylbutanoyl chloride were reacted to give the title compound in 83% yield. $[\alpha]_D^{20} = +2.55$ (c 2.9, CHCl_3); IR (neat) 3454 (OH), 2953 (CH), 1730 (C=O) cm^{-1} ; ^1H NMR (250 MHz, CDCl_3) δ 1.03 (d, $J = 6.6$ Hz, 6 H, $\text{C}(\text{O})\text{CH}_2\text{CHMe}_2$), 2.12–2.25 (m, 1 H, $\text{C}(\text{O})\text{CH}_2\text{CHMe}_2$), 2.30 (d, $J = 6.6$ Hz, 2 H, $\text{C}(\text{O})\text{CH}_2\text{CHMe}_2$), 2.61 (d, $J = 4.9$ Hz, 1 H, $\text{OCH}_2\text{CH}(\text{OH})\text{CH}_2\text{O}$), 3.61 (2 overlapping AB quartets, 2 H, $\text{OCH}_2\text{CH}(\text{OH})\text{CH}_2\text{O}$), 4.01–4.18 (m, 1 H, $\text{OCH}_2\text{CH}(\text{OH})\text{CH}_2\text{O}$), 4.23–4.27 (m, 2 H, $\text{OCH}_2\text{CH}(\text{OH})\text{CH}_2\text{O}$), 4.64 (s, 2 H, PhCH_2O), 7.42 (s, 5 H, PhCH_2O); ^{13}C NMR (62.5, CDCl_3) δ 22.32, 25.59, 43.12, 65.16, 68.73, 70.87, 73.36, 127.61, 127.69, 128.30, 137.56, 173.00; FAB-MS (m/z , rel intensity) 267 (MH^+ , 50), 91 (100). Anal. ($\text{C}_{15}\text{H}_{22}\text{O}_4$) C, H.

1-(3-Methylbut-2-enoyl)-3-benzyl-*sn*-glycerol. (R)-(+)-3-benzoyloxy-1,2-propanediol and 3-methylbut-2-enoyl chloride were reacted to give the title compound in 85% yield. $[\alpha]_D^{20} = +5.21$ (c 1.84, CHCl_3); IR (neat) 3459 (OH), 3031 and 2913 (CH), 1715 (C=O), 1652 (C=C) cm^{-1} ; ^1H NMR (250 MHz, CDCl_3) δ 1.98 and 2.25 (s, 6 H, $\text{C}(\text{O})\text{CH}=\text{CMe}_2$), 2.60 (br s, 1 H, $\text{OCH}_2\text{CH}(\text{OH})\text{CH}_2\text{O}$), 3.62 (2 overlapping AB quartets, 2 H, $\text{OCH}_2\text{CH}(\text{OH})\text{CH}_2\text{O}$), 4.10–4.20 (m, 1 H, $\text{OCH}_2\text{CH}(\text{OH})\text{CH}_2\text{O}$), 4.20–4.33 (m, 2 H, $\text{CH}_2\text{CH}(\text{OH})\text{CH}_2\text{O}$), 4.65 (s, 2 H, PhCH_2O), 5.79 (s, 1 H, $\text{C}(\text{O})\text{CH}=\text{CMe}_2$), 7.42 (s, 5 H, PhCH_2O); ^{13}C NMR (62.5 MHz, CDCl_3) δ 20.23, 27.36, 64.66, 68.88, 70.99, 73.35, 115.44, 127.59, 127.64, 128.29, 137.64, 157.46, 166.41. FAB-MS (m/z , rel intensity) 265 (MH^+ , 53), 91 (78), 83 (100). Anal. ($\text{C}_{15}\text{H}_{20}\text{O}_4 \cdot 0.16\text{H}_2\text{O}$) C, H.

1-(3-Isopropyl-4-methylpentanoyl)-3-benzyl-*sn*-glycerol. (R)-(+)-3-benzoyloxy-1,2-propanediol and 4-methyl-3-(isopropyl)pentanoyl chloride were reacted to give the title compound in 87% yield. $[\alpha]_D^{20} = +1.48$ (c 2.16, CHCl_3); IR (neat) 3452 (OH), 2956 (CH), 1733 (C=O) cm^{-1} ; ^1H NMR (250 MHz, CDCl_3) δ 0.89 and 0.98 (d, $J = 6.8$ Hz, 12 H, $\text{C}(\text{O})\text{CH}_2\text{CH}(\text{CHMe}_2)_2$), 1.63–1.93 (m, 3 H, $\text{C}(\text{O})\text{CH}_2\text{CH}(\text{CHMe}_2)_2$), 2.29 (d, $J = 5.9$ Hz, 2 H, $\text{C}(\text{O})\text{CH}_2\text{CH}(\text{CHMe}_2)_2$), 3.61 (2 overlapping AB quartets, 2 H, $\text{OCH}_2\text{CH}(\text{OH})\text{CH}_2\text{O}$), 4.05–4.31 (m, 3 H, $\text{OCH}_2\text{CH}(\text{OH})\text{CH}_2\text{O}$), 4.64 (s, 2 H, PhCH_2O), 7.42 (s, 5 H, PhCH_2O); ^{13}C NMR (62.5 MHz, CDCl_3) δ 18.70, 21.31, 29.33, 32.79, 46.69, 65.35, 68.77, 70.90, 73.38, 127.61, 127.70, 128.31, 137.52, 174.80. FAB-MS (m/z , rel intensity) 323 (MH^+ , 29), 91 (100). Anal. ($\text{C}_{19}\text{H}_{30}\text{O}_4$) C, H.

1-[4-Methyl-3-(isopropyl)pent-2-enoyl]-3-benzyl-*sn*-glycerol. (R)-(+)-3-benzoyloxy-1,2-propanediol and 4-methyl-3-(isopropyl)pent-2-enoyl chloride were reacted to give the title compound in 58% yield. $[\alpha]_D^{20} = +3.88$ (c 3.07 CHCl_3); IR (neat) 3415 (OH), 2964 (CH), 2871 (CH), 1714 (C=O), 1637 (C=C) cm^{-1} ; ^1H NMR (250 MHz, CDCl_3) δ 1.14 (d, $J = 6.8$ Hz, 6 H, $\text{C}(\text{O})\text{CH}=\text{C}(\text{CHMe}_2)_2$), 1.16 (d, $J = 6.6$ Hz, 6 H, $\text{C}(\text{O})\text{CH}=\text{C}(\text{CHMe}_2)_2$), 2.59 (br s, 1 H, $\text{OCH}_2\text{CH}(\text{OH})\text{CH}_2\text{O}$), 2.64 (heptet, $J = 6.8$ Hz, 2 H, $\text{C}(\text{O})\text{CH}=\text{C}(\text{CHMe}_2)_2$), 3.63 (2 overlapping AB quartets, 2 H, $\text{OCH}_2\text{CH}(\text{OH})\text{CH}_2\text{O}$), 4.07–4.33 (m, 3 H, $\text{OCH}_2\text{CH}(\text{OH})\text{CH}_2\text{O}$), 4.66 (s, 2 H, PhCH_2O), 5.76 (s, 1 H, $\text{C}(\text{O})\text{CH}=\text{C}(\text{CHMe}_2)_2$), 7.42 (s, 5 H, PhCH_2O); ^{13}C NMR (62.5 MHz, CDCl_3) δ 20.22, 24.11, 28.98, 29.70, 64.76, 68.89, 71.01, 73.33, 112.15, 127.57, 127.64, 128.28, 137.65, 166.79, 176.88. FAB-MS (m/z , rel intensity) 321 (MH^+ , 54), 139 (100), 91 (57). Anal. ($\text{C}_{19}\text{H}_{28}\text{O}_4$) C, H.

General Procedure for the Synthesis of 1,2-Disubstituted-3-benzyl Glycerols. Under argon, pyridine (4.0 equiv) and DMAP (0.1 equiv) were added to a stirring solution of

1-acyl-3-benzyl-*sn*-glycerol (1.0 equiv) in CH_2Cl_2 (10 mL/mmol). The mixture was then cooled to 0 °C, and acyl chloride (4.0 equiv) was added dropwise. The ice bath was removed, and the reaction was warmed to room temperature and was monitored by TLC. The crude reaction was then filtered through a plug of silica gel and concentrated. Further purification by silica gel column chromatography (5% ether/hexane) gives the named product as a colorless oil.

1-(3-Methylbutanoyl)-2-(3-methylbut-2-enoyl)-3-benzyl-*sn*-glycerol. (R)-(+)-1-(3-methylbutanoyl)-3-benzyl-*sn*-glycerol and 3-methylbut-2-enoyl chloride were reacted to give the title compound in 32% yield. $[\alpha]_D^{20} = +11.34$ (c 0.67, CHCl_3); IR (neat) 2959 (CH), 1735 (C=O), 1721 (C=O), 1654 (C=C) cm^{-1} ; ^1H NMR (250 MHz, CDCl_3) δ 1.01 (d, $J = 6.4$ Hz, 6 H, $\text{C}(\text{O})\text{CH}_2\text{CHMe}_2$), 1.98 (d, $J = 1.2$ Hz, 3 H, $\text{C}(\text{O})\text{CH}=\text{CMe}_2$), 2.05–2.35 (m, 3 H, $\text{C}(\text{O})\text{CH}_2\text{CHMe}_2$ containing δ 2.25 (d, $J = 1.2$ Hz, 3 H, $\text{C}(\text{O})\text{CH}=\text{CMe}_2$), 3.70 (d, $J = 5.4$ Hz, 2 H, $\text{OCH}_2\text{CH}(\text{O}-)\text{CH}_2\text{O}$), 4.25–4.50 (m, 2 H, $\text{OCH}_2\text{CH}(\text{O}-)\text{CH}_2\text{O}$), 4.63 (AB quartet, $J = 9.3$ Hz, 2 H, PhCH_2O), 5.30–5.38 (m, 1 H, $\text{OCH}_2\text{CH}(\text{O}-)\text{CH}_2\text{O}$), 5.78 (t, $J = 1.2$ Hz, 1H, $\text{C}(\text{O})\text{CH}=\text{CMe}_2$), 7.39 (s, 5 H, PhCH_2O); ^{13}C NMR (62.5 MHz, CDCl_3) δ 20.26, 22.31, 25.57, 27.41, 43.13, 62.60, 68.23, 69.12, 73.21, 115.53, 127.50, 127.58, 128.25, 137.64, 157.66, 165.46, 172.53. FAB-MS (m/z , relative intensity) 349 (MH^+ , 36), 91 (71), 83 (100). HRMS (FAB) calcd for $\text{C}_{20}\text{H}_{29}\text{O}_5$ (MH^+): 349.2015, found 349.2021.

1-(3-Methylbutanoyl)-2-(3-isopropyl-4-methylpentanoyl)-3-benzyl-*sn*-glycerol. According to the general procedure, 1-(3-methylbutanoyl)-3-benzyl-*sn*-glycerol and 3-isopropyl-4-methylpentanoyl chloride were reacted to give the title compound in 56% yield. $[\alpha]_D^{20} = +11.9$ (c 2.7, CHCl_3); IR (neat) 2963 (CH), 2871 (CH), 1739 (C=O) cm^{-1} ; ^1H NMR (250 MHz, CDCl_3) δ 0.89 (dd, $J = 6.6$, 1.5 Hz, 6 H, $\text{C}(\text{O})\text{CH}_2\text{CH}(\text{CHMe}_2)_2$), 0.99 (d, $J = 6.6$ Hz, 6 H, $\text{C}(\text{O})\text{CH}_2\text{CH}(\text{CHMe}_2)_2$), 1.02 (d, $J = 6.3$ Hz, 6 H, $\text{C}(\text{O})\text{CH}_2\text{CHMe}_2$), 1.66–1.91 (m, 3 H, $\text{C}(\text{O})\text{CH}_2\text{CH}(\text{CHMe}_2)_2$), 2.09–2.33 (m, 1 H, $\text{C}(\text{O})\text{CH}_2\text{CHMe}_2$ containing δ 2.25 (d, $J = 6.1$ Hz, 2 H, $\text{C}(\text{O})\text{CH}_2\text{CH}(\text{CHMe}_2)_2$) and δ 2.28 (d, $J = 5.6$ Hz, 2 H, $\text{C}(\text{O})\text{CH}_2\text{CHMe}_2$), 3.68 (d, $J = 4.9$ Hz, 2 H, $\text{OCH}_2\text{CH}(\text{O}-)\text{CH}_2\text{O}$), 4.28 (dd, $J = 11.8$, 6.5 Hz, 1 H, $\text{OCH}_2\text{CH}(\text{O}-)\text{CH}_2\text{O}$), 4.44 (dd, $J = 12.0$, 3.7 Hz, 1 H, $\text{OCH}_2\text{CH}(\text{O}-)\text{CH}_2\text{O}$), 4.62 (AB quartet, $J = 12.1$ Hz, 2 H, PhCH_2O), 5.28–5.36 (m, 1 H, $\text{OCH}_2\text{CH}(\text{O}-)\text{CH}_2\text{O}$), 7.40 (s, 5 H, PhCH_2O); ^{13}C NMR (62.5 MHz, CDCl_3) δ 18.67, 18.70, 21.28, 21.30, 22.31, 25.53, 29.29, 29.35, 32.94, 43.07, 46.61, 62.54, 68.15, 69.96, 73.17, 127.46, 127.58, 128.23, 137.56, 172.38, 173.86; FAB-MS (m/z , relative intensity) 407 (MH^+ , 9), 91 (100). Anal. ($\text{C}_{24}\text{H}_{38}\text{O}_5$) C, H.

1-(3-Methylbutanoyl)-2-(3-isopropyl-4-methylpent-2-enoyl)-3-benzyl-*sn*-glycerol. According to the general procedure, 1-(3-methylbutanoyl)-3-benzyl-*sn*-glycerol and 3-isopropyl-4-methylpentanoyl chloride were reacted to give the title compound in 77% yield. $[\alpha]_D^{20} = +7.23$ (c 4.73, CHCl_3); IR (neat) 2963 (CH), 2871 (CH), 1740 (C=O), 1719 (C=O), 1637 (C=C) cm^{-1} ; ^1H NMR (250 MHz, CDCl_3) δ 1.01 (d, $J = 6.6$ Hz, 6 H, $\text{C}(\text{O})\text{CH}_2\text{CHMe}_2$), 1.13 (d, $J = 6.9$ Hz, 6 H, $\text{C}(\text{O})\text{CH}=\text{C}(\text{CHMe}_2)_2$), 1.15 (d, $J = 6.3$ Hz, 6 H, $\text{C}(\text{O})\text{CH}=\text{C}(\text{CHMe}_2)_2$), 2.08–2.33 (m, 3 H, $\text{C}(\text{O})\text{CH}_2\text{CHMe}_2$), 2.63 (heptet, $J = 6.7$ Hz, 1 H, $\text{C}(\text{O})\text{CH}=\text{C}(\text{CHMe}_2)_2$), 3.71 (d, $J = 5.1$, 2 H, $\text{OCH}_2\text{CH}(\text{O}-)\text{CH}_2\text{O}$), 4.12 (heptet, $J = 6.8$ Hz, 1 H, $\text{C}(\text{O})\text{CH}=\text{C}(\text{CHMe}_2)_2$), 4.25–4.50 (m, 2 H, $\text{OCH}_2\text{CH}(\text{O}-)\text{CH}_2\text{O}$), 4.62 (AB quartet, $J = 9.7$ Hz, 2 H, PhCH_2O), 5.29–5.40 (m, 1 H, $\text{OCH}_2\text{CH}(\text{O}-)\text{CH}_2\text{O}$), 5.74 (s, 1 H, $\text{C}(\text{O})\text{CH}=\text{C}(\text{CHMe}_2)_2$), 7.38 (s, 5 H, PhCH_2O); ^{13}C NMR (62.5 MHz, CDCl_3) δ 20.18, 21.22, 22.30, 24.08, 25.57, 29.00, 29.74, 43.14, 62.57, 68.21, 69.06, 73.16, 112.25, 127.45, 127.48, 127.56, 128.23, 137.63, 165.84, 172.44, 176.98; FAB-MS (m/z , relative intensity) 405 (MH^+ , 22), 139 (100), 91 (91). Anal. ($\text{C}_{24}\text{H}_{36}\text{O}_5 \cdot 0.2 \text{H}_2\text{O}$) C, H.

1-(3-Methylbut-2-enoyl)-2-(3-methylbutanoyl)-3-benzyl-*sn*-glycerol. According to the general procedure, 1-(3-methylbut-2-enoyl)-3-benzyl-*sn*-glycerol and isovaleryl chloride were reacted to give the title compound in 80% yield. $[\alpha]_D^{20} = +9.29$ (c 5.31, CHCl_3); IR (neat) 2959 (CH), 2871 (CH), 1736 (C=O), 1723 (C=O), 1654 (C=C) cm^{-1} ; ^1H NMR (250 MHz, CDCl_3) δ 1.03 (d, $J = 6.4$ Hz, 6 H, $\text{C}(\text{O})\text{CH}_2\text{CHMe}_2$), 1.96 (s, 3 H, $\text{C}(\text{O})$ -

CH=CM₂), 2.12–2.30 (m, 3 H, C(O)CH₂CHMe₂ containing δ 2.23 (s, 3 H, C(O)CH=CM₂), 3.69 (d, J = 5.1 Hz, 2 H, OCH₂CH(O–)CH₂O), 4.36 (2 overlapping AB quartets, 2 H, OCH₂CH(O–)CH₂O), 4.61 (AB quartet, J = 7.3 Hz, 2 H, PhCH₂O), 5.32–5.40 (m, 1 H, OCH₂CH(O–)CH₂O), 5.72 (s, 1 H, C(O)CH=CM₂), 7.40 (s, 5 H, PhCH₂O); ¹³C NMR (62.5 MHz, CDCl₃) δ 20.18, 22.26, 25.67, 27.33, 43.34, 61.92, 68.33, 70.01, 73.15, 115.38, 127.46, 127.56, 128.23, 137.62, 157.26, 165.84, 172.13; FAB-MS (m/z , relative intensity): 349 (MH⁺, 27), 91 (94), 83 (100). Anal. (C₂₀H₂₈O₅) C, H.

1,2-Di-(3-methylbut-2-enoyl)-3-benzyl-sn-glycerol. According to the general procedure, (R)-(+)-3-benzoyloxy-1,2-propanediol and 3,3-dimethylacryloyl chloride (3 equiv) were reacted to give the title compound in quantitative yield. [α]_D²⁰ = +3.59 (c 1.95, CHCl₃); IR (neat) 2914 (CH), 1721 (C=O), 1652 (C=C) cm⁻¹; ¹H NMR (250 MHz, CDCl₃) δ 1.97 (d, J = 1.2 Hz, 3 H, C(O)CH=CM₂), 1.98 (d, J = 1.3 Hz, 3 H, C(O)CH=CM₂), 2.23 and 2.25 (d, J = 1.2 Hz, 6 H, C(O)CH=CM₂), 3.72 (d, J = 5.2 Hz, 2 H, OCH₂O(O–)CH₂O), 4.34 (dd, J = 11.8, 6.1 Hz, 1 H, OCH₂CH(O–)CH₂O), 4.44 (dd, J = 11.8, 4.2 Hz, 1 H, OCH₂CH(O–)CH₂O), 4.63 (AB quartet, J = 9.3 Hz, 2 H, PhCH₂O), 5.32–5.40 (m, 1 H, OCH₂CH(O–)CH₂O), 5.73–5.75 (m, J = 1.3 Hz, 1 H, C(O)CH=CM₂), 5.78–5.80 (m, J = 1.3 Hz, 1 H, C(O)CH=CM₂), 7.40 (s, 5 H, PhCH₂O); ¹³C NMR (62.5 MHz, CDCl₃) δ 20.17, 20.22, 27.30, 27.34, 62.04, 68.35, 69.33, 73.16, 115.52, 115.67, 127.45, 127.49, 128.20, 137.73, 157.02, 157.39, 165.46, 165.90. FABMS (m/z , relative intensity): 347 (MH⁺, 42), 247 (100), 91 (97), 83 (100). Anal. (C₂₀H₂₆O₅) C, H.

1-(3-Methylbut-2-enoyl)-2-(3-isopropyl-4-methylpentanoyl)-3-benzyl-sn-glycerol. According to the general procedure, 1-(3-methylbut-2-enoyl)-3-benzyl-sn-glycerol and 3-isopropyl-4-methylpentanoyl chloride were reacted to give the title compound in 40% yield. [α]_D²⁰ = +9.80 (c 1.53, CHCl₃); IR (neat) 2960 (CH), 2874 (CH), 1727 (C=O), 1653 (C=C) cm⁻¹; ¹H NMR (250 MHz, CDCl₃) δ 0.89 and 1.01 (d, J = 6.6 Hz, 12 H, C(O)CH₂CH(CHMe₂)₂), 1.71 (pentet, J = 5.7 Hz, 1 H, C(O)CH₂CH(CHMe₂)₂), 1.81 (heptet, J = 6.6 Hz, 2 H, C(O)CH₂CH(CHMe₂)₂), 1.97 and 2.23 (d, J = 0.7 Hz, 6 H, C(O)CH=CM₂), 2.29 (d, 2 H, J = 5.6 Hz, C(O)CH₂CH(CHMe₂)₂), 3.70 (d, J = 5.1 Hz, 2 H, OCH₂CH(O–)CH₂O), 4.32 (dd, J = 12.0, 6.3 Hz, 1 H, OCH₂CH(O–)CH₂O), 4.42 (dd, J = 12.0, 3.9 Hz, 1 H, OCH₂CH(O–)CH₂O), 4.60 (AB quartet, J = 8.1 Hz, 2 H, PhCH₂O), 5.31–5.39 (m, 1 H, OCH₂CH(O–)CH₂O), 5.72 (s, 1 H, C(O)CH=CM₂), 7.40 (s, 5 H, PhCH₂O); ¹³C NMR (62.5 MHz, CDCl₃) δ 18.69, 18.71, 20.20, 21.27, 27.34, 29.29, 29.35, 33.00, 46.63, 61.94, 68.31, 70.09, 73.18, 115.41, 127.45, 127.54, 128.23, 137.64, 157.21, 165.91, 173.96. FABMS (m/z , relative intensity): 405 (MH⁺, 14), 91 (72), 83 (100). Anal. (C₂₄H₃₆O₅) C, H.

1-(3-Methylbut-2-enoyl)-2-(3-isopropyl-4-methylpent-2-enoyl)-3-benzyl-sn-glycerol. Under argon, DCC (0.35 g, 1.70 mmol), DMAP (0.14 g, 1.14 mmol), and a solution of 1-(3-methylbut-2-enoyl)-3-benzyl-sn-glycerol (0.33 g, 1.13 mmol) in toluene (4 mL) were added to a solution of 3-isopropyl-4-methylpent-2-enoic acid (0.27 g, 1.7 mmol) in toluene (8 mL) and heated to 80 °C for 3 h. After cooling to room temperature, the crude reaction mixture was concentrated to dryness in vacuo, dissolved in Et₂O, and recrystallized. Purification by silica gel chromatography (gradient elution from 5% EtOAc in hexane to 25% EtOAc in hexane) gave the title compound contaminated by DCC/DCU which was used directly as in the next step without further purification.

1-(3-Isopropyl-4-methylpentanoyl)-2-(3-methylbutanoyl)-3-benzyl-sn-glycerol. According to the general procedure, 1-(3-isopropyl-4-methylpentanoyl)-3-benzyl-sn-glycerol and isovaleryl chloride were reacted to give the title compound in 88% yield. [α]_D²⁰ = +8.57 (c 1.54, CHCl₃); IR (neat) 2960 (CH), 2873 (CH), 1740 (C=O) cm⁻¹; ¹H NMR (250 MHz, CDCl₃) δ 0.88 and 0.97 (d, J = 6.8 Hz, 12 H, C(O)CH₂CH(CHMe₂)₂), 1.04 (d, J = 6.4 Hz, 6 H, C(O)CH₂CH(CHMe₂)₂), 1.63–1.72 (m, J = 5.7 Hz, 1 H, C(O)CH₂CH(CHMe₂)₂), 1.80 (heptet, J = 6.6 Hz, 2 H, C(O)CH₂CH(CHMe₂)₂), 2.13–2.33 (m, 5 H, C(O)CH₂CH(CHMe₂)₂ and C(O)CH₂CHMe₂), 3.68 (d, J = 5.1 Hz, 2 H, OCH₂CH(O–)CH₂O), 4.26 (dd, J = 12.0, 6.6 Hz, 1 H, OCH₂CH(O–)CH₂O), 4.43 (dd, J = 11.8, 3.8 Hz, 1 H, OCH₂CH(O–)CH₂O), 4.62 (AB quartet, J = 7.1 Hz, 2 H, PhCH₂O), 5.30–5.38 (m, 1 H, OCH₂CH(O–)CH₂O), 7.34–7.43 (m, 5 H, PhCH₂O); ¹³C NMR (62.5 MHz, CDCl₃) δ 18.68, 21.29, 22.29, 25.67, 29.30, 32.75, 43.32, 46.66, 62.75, 68.25, 69.87, 73.21, 127.49, 127.62, 128.27, 137.53, 172.16, 174.26; FABMS (m/z , relative intensity): 407 (MH⁺, 11), 91 (99), 57 (100). Anal. (C₂₄H₃₈O₅) C, H.

1-(3-Isopropyl-4-methylpentanoyl)-2-(3-methylbut-2-enoyl)-3-benzyl-sn-glycerol. According to the general procedure, 1-(3-isopropyl-4-methylpentanoyl)-3-benzyl-sn-glycerol and 3,3-dimethylacryloyl chloride were reacted to give the title compound contaminated by (CH₃)₂C=CHCOOH (ca. 1:1) in 74% yield. This product was used directly in the next step without further purification.

1,2-Di-(3-isopropyl-4-methylpentanoyl)-3-benzyl-sn-glycerol. Under argon, 3-isopropyl-4-methylpent-2-enoyl chloride was added to a 0 °C solution of 3-isopropyl-4-methylpentanoyl chloride in CH₂Cl₂ and stirred overnight warming to room temperature. The crude reaction mixture was then concentrated in vacuo, and the products were separated by column chromatography to give the desired title compound in 64% yield, along with the monoacylated product in 33% yield. This compound was used directly in the next step without further purification. ¹H NMR (250 MHz, CDCl₃) δ 0.87–1.03 (m, 24 H, C(O)CH₂CH(CHMe₂)₂), 1.52–1.90 (m, 6 H, C(O)CH₂CH(CHMe₂)₂), 2.24 (d, J = 5.9 Hz, 2 H, C(O)CH₂CH(CHMe₂)₂), 2.28 (d, J = 5.6 Hz, 2 H, C(O)CH₂CH(CHMe₂)₂), 3.69 (d, J = 5.1 Hz, 2 H, OCH₂CH(O–)CH₂O), 4.27 (dd, J = 12.0, 6.3, 1 H, OCH₂CH(O–)CH₂O), 4.43 (dd, J = 12.0, 3.8, 1 H, OCH₂CH(O–)CH₂O), 4.62 (AB quartet, J = 7.3 Hz, PhCH₂O), 5.30–5.38 (m, 1 H, OCH₂CH(O–)CH₂O), 7.40 (s, 5 H, PhCH₂O); ¹³C NMR (62.5 MHz, CDCl₃) δ 18.68, 21.29, 29.31, 32.70, 32.94, 46.62, 62.72, 68.19, 69.96, 73.18, 127.44, 127.56, 128.23, 137.56, 173.84, 174.16.

1-(3-Isopropyl-4-methylpentanoyl)-2-(3-isopropyl-4-methylpent-2-enoyl)-3-benzyl-sn-glycerol. According to the general procedure, 1-(3-isopropyl-4-methylpentanoyl)-3-benzyl-sn-glycerol and 3-isopropyl-4-methylpent-2-enoyl chloride were reacted to give the title compound in 36% yield. [α]_D²⁰ = +7.89 (c = 0.71, CHCl₃); IR (neat) 2961 (CH), 2360 (CH), 1728 (C=O), 1637 (C=C) cm⁻¹; ¹H NMR (250 MHz, CDCl₃) δ 0.88 (d, J = 6.8 Hz, 6 H, C(O)CH₂CH(CHMe₂)₂), 0.97 (d, J = 6.6 Hz, 6 H, C(O)CH₂CH(CHMe₂)₂), 1.15 (irreg t, 12 H, C(O)CH=CH(CHMe₂)₂), 1.60–1.75 (m, 1 H, C(O)CH₂CH(CHMe₂)₂), 1.75–1.90 (m, 2 H, C(O)CH₂CH(CHMe₂)₂), 2.25 (d, J = 5.6 Hz, 2 H, C(O)CH₂CH(CHMe₂)₂), 2.64 (heptet, J = 6.8 Hz, 1 H, C(O)CH=CH(CHMe₂)₂), 3.72 (d, J = 5.1 Hz, 2 H, OCH₂CH(O–)CH₂O), 4.13 (heptet, J = 6.8 Hz, 1 H, C(O)CH=CH(CHMe₂)₂), 4.32 (dd, J = 11.8, 6.2 Hz, 1 H, OCH₂CH(O–)CH₂O), 4.43 (dd, J = 11.8, 3.9 Hz, 1 H, OCH₂CH(O–)CH₂O), 4.64 (AB quartet, J = 10.8 Hz, 2 H, PhCH₂O), 5.30–5.40 (m, 1 H, OCH₂CH(O–)CH₂O), 5.75 (s, 1 H, C(O)CH=CH(CHMe₂)₂), 7.40 (s, 5 H, PhCH₂O); ¹³C NMR (62.5 MHz, CDCl₃) δ 18.66, 18.71, 20.22, 21.30, 21.31, 24.09, 29.03, 29.30, 29.35, 29.76, 32.82, 46.73, 62.80, 68.31, 69.09, 73.19, 112.27, 127.47, 127.56, 128.24, 137.66, 165.86, 174.27, 177.00; FAB-MS (m/z , relative intensity): 461 (MH⁺, 7), 139 (100), 91 (46). Anal. (C₂₈H₄₄O₅) C, H.

1-(3-Isopropyl-4-methylpent-2-enoyl)-2-(3-methylbutanoyl)-3-benzyl-sn-glycerol. According to the general procedure, 1-(3-isopropyl-4-methylpent-2-enoyl)-3-benzyl-sn-glycerol and isovaleryl chloride were reacted to give the title compound in 85% yield. [α]_D²⁰ = +8.08 (c 2.53, CHCl₃); IR (neat) 2963 (CH), 2871 (CH), 1740 (C=O), 1719 (C=O), 1637 (C=C) cm⁻¹; ¹H NMR (250 MHz, CDCl₃) δ 1.03 (d, J = 6.4 Hz, 6 H, C(O)CH₂CH(CHMe₂)₂), 1.13 and 1.14 (d, J = 6.8 Hz, 12 H, C(O)CH=CH(CHMe₂)₂), 2.21 (heptet, J = 6.6 Hz, 1 H, C(O)CH=CH(CHMe₂)₂), 2.30 (d, J = 6.4 Hz, 2 H, C(O)CH₂CH(CHMe₂)₂), 2.62 (heptet, J = 6.8 Hz, 1 H, C(O)CH=CH(CHMe₂)₂), 3.69 (d, J = 4.9 Hz, 2 H, OCH₂CH(O–)CH₂O), 4.11 (heptet, J = 6.8 Hz, 1 H, C(O)CH=CH(CHMe₂)₂), 4.31 (dd, J = 12.0, 6.6 Hz, 1 H, OCH₂CH(O–)CH₂O), 4.41 (dd, J = 12.0, 4.0 Hz, 1 H, OCH₂CH(O–)CH₂O), 4.62 (AB quartet, J = 7.7 Hz, 2 H, PhCH₂O), 5.33–5.41 (m, 1 H, OCH₂CH(O–)CH₂O), 5.69 (s, 1 H, C(O)CH=

(CHMe₂)₂, 7.39 (s, 5 H, PhCH₂O); ¹³C NMR (62.5 MHz, CDCl₃) δ 20.21, 22.26, 24.09, 25.69, 28.94, 29.71, 43.36, 61.97, 68.36, 70.01, 73.15, 112.09, 127.44, 127.56, 128.23, 137.63, 166.27, 172.10, 176.64; FAB-MS (*m/z*, relative intensity): 403 (MH⁺, 9), 139 (100), 91 (55). Anal. (C₂₄H₃₆O₅) C, H.

1-(3-Isopropyl-4-methylpent-2-enoyl)-2-(3-methylbut-2-enoyl)-3-benzyl-*sn*-glycerol. According to the general procedure, 1-(3-isopropyl-4-methylpent-2-enoyl)-3-benzyl-*sn*-glycerol and 3,3-dimethylacryloyl chloride were reacted to give the title compound in 70% yield. [α]_D²⁰ +4.22 (*c* 2.02, CHCl₃); IR (neat) 2965 (CH), 2870 (CH), 1719 (C=O), 1654 (C=C), 1637 (C=C) cm⁻¹; ¹H NMR (250 MHz, CDCl₃) δ 1.14 (t, *J* = 6.6 Hz, 12 H, C(O)CH=C(CHMe₂)₂), 1.98 (d, *J* = 0.7 Hz, 3 H, C(O)CH=CMe₂), 2.25 (d, *J* = 1.0 Hz, 3 H, C(O)CH=CMe₂), 2.63 (heptet, *J* = 6.8 Hz, 1 H, C(O)CH=C(CHMe₂)₂), 3.73 (d, *J* = 5.1 Hz, 2 H, OCH₂CH(O-)CH₂O), 4.10 (heptet, *J* = 6.8 Hz, 1 H, C(O)CH=C(CHMe₂)₂), 4.34 (dd, *J* = 11.8, 6.0 Hz, 1 H, OCH₂CH(O-)CH₂O), 4.43 (dd, *J* = 11.8, 4.2 Hz, 1 H, OCH₂CH(O-)CH₂O), 4.64 (AB quartet, *J* = 9.7 Hz, 2 H, PhCH₂O), 5.33–5.41 (m, 1 H, OCH₂CH(O-)CH₂O), 5.71 (s, 1 H, C(O)CH=C(CHMe₂)₂), 5.81 (irreg t, 1H, C(O)CH=CMe₂), 7.40 (s, 5 H, PhCH₂O); ¹³C NMR (62.5 MHz, CDCl₃) δ 20.22, 20.25, 24.12, 27.38, 28.92, 29.75, 62.10, 68.35, 69.37, 73.17, 112.21, 115.67, 127.46, 127.52, 128.23, 137.73, 157.44, 165.51, 166.44, 176.45; FAB-MS (*m/z*, relative intensity): 403 (MH⁺, 7), 139 (100), 91 (42). Anal. (C₂₄H₃₄O₅) C, H.

1-(3-Isopropyl-4-methylpent-2-enoyl)-2-(3-isopropyl-4-methylpentanoyl)-3-benzyl-*sn*-glycerol. According to the general procedure, 1-(3-isopropyl-4-methylpent-2-enoyl)-3-benzyl-*sn*-glycerol and 3-isopropyl-4-methylpentanoyl chloride were reacted to give the title compound in 40% yield. [α]_D²⁰ +8.18 (*c* 1.04, CHCl₃); IR (neat) 2963 (CH), 2873 (CH), 1735 (C=O), 1719 (C=O), 1637 (C=C) cm⁻¹; ¹H NMR (250 MHz, CDCl₃) δ 0.89 (dd, *J* = 6.7, 0.6 Hz, 6 H, C(O)CH₂CH(CHMe₂)₂), 0.99 (d, *J* = 6.8 Hz, 6 H, C(O)CH₂CH(CHMe₂)₂), 1.13 and 1.15 (d, *J* = 6.8 Hz, 12 H, C(O)CH=C(CHMe₂)₂), 1.72 (pentet, *J* = 5.7 Hz, 1 H C(O)CH₂CH(CHMe₂)₂), 1.82 (heptet, 2 H, C(O)CH₂CH(CHMe₂)₂), 2.29 (d, *J* = 5.6 Hz, 2 H, C(O)CH₂CH(CHMe₂)₂), 2.63 (heptet, *J* = 6.8 Hz, 1 H, C(O)CH=C(CHMe₂)₂), 3.71 (d, *J* = 5.1 Hz, 2 H, OCH₂CH(O-)CH₂O), 4.12 (heptet, *J* = 6.8 Hz, 1 H, C(O)CH=C(CHMe₂)₂), 4.31 (dd, *J* = 12.0, 6.6 Hz, 1 H, OCH₂CH(O-)CH₂O), 4.42 (dd, *J* = 12.0, 3.9 Hz, 1 H, OCH₂CH(O-)CH₂O), 4.63 (AB quartet, *J* = 9.0 Hz, 2 H, PhCH₂O), 5.31–5.40 (m, 1 H, OCH₂CH(O-)CH₂O), 5.69 (s, 1 H, C(O)CH=C(CHMe₂)₂), 7.40 (s, 5 H, PhCH₂O); ¹³C NMR (62.5 MHz, CDCl₃) δ 18.68, 18.73, 20.22, 21.32, 24.11, 28.93, 29.31, 29.38, 29.71, 33.01, 46.67, 62.00, 68.32, 70.13, 73.15, 112.07, 127.45, 127.56, 128.24, 137.65, 166.34, 173.98, 176.74; FAB-MS (*m/z*, relative intensity): 461 (MH⁺, 9), 139 (100), 91 (100). Anal. (C₂₈H₄₄O₅) C, H.

1,2-Di-(3-isopropyl-4-methylpent-2-enoyl)-3-benzyl-*sn*-glycerol. Under argon, a solution of (R)-(+)-3-benzoyloxy-1,2-propanediol (1.0 g, 5.49 mmol) in toluene (4 mL) was added to a solution of 4-methyl-3-(isopropyl)pent-2-enoic acid (2.17 g, 13.71 mmol, 2.5 equiv) in toluene (38.4 mL) containing DCC (2.83 g, 13.72 mmol, 2.5 equiv) and DMAP (1.34 g, 10.96 mmol, 2 equiv). The mixture was heated at 80 °C for 3 h and then concentrated under reduced pressure. The residue was recrystallized from Et₂O several times to partially eliminate DCC/DCU. Further purification by silica gel chromatography (gradient elution from 2% EtOAc in hexane to 25% EtOAc in hexane) gave the title compound (0.36 g, 0.79 mmol, 58%) along with two other monoacylated products (0.964 and 0.23 g). [α]_D²⁰ = +6.19 (*c* 1.68, CHCl₃); IR (neat) 2964 (CH), 2874 (CH), 1718 (C=O), 1637 (C=C) cm⁻¹; ¹H NMR (250 MHz, CDCl₃) δ 1.10–1.20 (m, 24 H, C(O)CH=C(CHMe₂)₂), 2.63 and 2.64 (heptet, *J* = 6.8 Hz, 2 H, C(O)CH=C(CHMe₂)₂), 3.74 (d, *J* = 5.1 Hz, 2 H, OCH₂CH(O-)CH₂O), 4.00–4.21 (m, 2 H, C(O)CH=C(CHMe₂)₂), 4.35 (dd, *J* = 12.0, 5.9 Hz, 1 H, OCH₂CH(O-)CH₂O), 4.43 (dd, *J* = 12.0, 4.3 Hz, 1 H, OCH₂CH(O-)CH₂O), 4.65 (AB quartet, *J* = 9.4 Hz, 2 H, PhCH₂O), 5.32–5.40 (m, 1 H, OCH₂CH(O-)CH₂O), 5.71 and 5.77 (s, 1 H, C(O)CH=C(CHMe₂)₂), 7.40 (s, 5H, PhCH₂O-); ¹³C NMR (62.5 MHz, CDCl₃) δ 20.22, 20.25, 24.10, 28.95, 29.05, 29.78, 62.10,

68.34, 69.35, 73.15, 112.24, 112.38, 127.46, 127.52, 128.23, 137.75, 165.96, 166.44, 176.39, 176.78. FAB-MS (*m/z*, relative intensity): 459 (MH⁺, 11), 139 (100), 91 (97). Anal. (C₂₈H₄₂O₅) C, H.

General Procedure for the Debenzylation of Unsaturated 1,2-Disubstituted-3-benzyl Glycerols. Under argon, BCl₃ (4.0 equiv) was added dropwise to a -78 °C stirring solution of 1,2-disubstituted-3-benzyl-*sn*-glycerol (1.0 equiv) in CH₂Cl₂ (40 mL/mmol). The reaction was monitored by TLC and complete within 1–2 h. The reaction was then diluted with Et₂O (40 mL/mmol) and poured into a pH = 7 buffer solution. After washing with a pH = 7 buffer solution (3×), the organic layer was dried over MgSO₄ and concentrated. Purification by silica gel column chromatography (3 hexane:1 Et₂O) gives the named product as a colorless oil.

1,2-Di-(3-methylbutanoyl)-*sn*-glycerol (1A). Palladium on carbon (50 mg, 10%) was added to a solution of 1,2-di-(3-methylbut-2-enoyl)-3-benzyl-*sn*-glycerol (0.5 g, 1.44 mmol) in methanol (20 mL), and the mixture was agitated under H₂ pressure (44 psi) for 2 h. The palladium was filtered off, and the filtrate was concentrated under reduced pressure. Purification by silica gel chromatography (gradient elution from 20% EtOAc/hexane to 30% EtOAc/hexane) gave **1A** (375 mg, 1.44 mmol, 100%). [α]_D²⁰ = -3.92 (*c* 3.34, CHCl₃); IR (neat) 3467 (OH), 2961 (CH), 2874 (CH), 1740 (C=O) cm⁻¹; ¹H NMR (250 MHz, CDCl₃) δ 1.03 (d, *J* = 2.7 Hz, 6 H, C(O)CH₂CHMe₂), 1.05 (d, *J* = 2.4 Hz, 6 H, C(O)CH₂CHMe₂), 2.05–2.35 (m, 6 H, C(O)CH₂CHMe₂), 3.81 (d, *J* = 5.1 Hz, 2 H, HOCH₂CH(O-)CH₂O), 4.30 (dd, *J* = 12.0, 5.6 Hz, 1 H, HOCH₂CH(O-)CH₂O), 4.41 (dd, *J* = 12.0, 4.4 Hz, 1 H, HOCH₂CH(O-)CH₂O), 5.17 (m, 1 H, HOCH₂CH(O-)CH₂O); ¹³C NMR (62.5 MHz, CDCl₃) δ 22.19, 22.24, 25.51, 25.61, 43.03, 43.22, 61.20, 62.08, 71.91, 172.52, 172.82. FAB-MS (*m/z*, relative intensity): 261 (MH⁺, 36), 159 (100), 85 (100). Anal. (C₁₃H₂₄O₅) C, H.

1-(3-Methylbutanoyl)-2-(3-methylbut-2-enoyl)-*sn*-glycerol (1B). According to the general procedure, 1-(3-methylbutanoyl)-2-(3-methylbut-2-enoyl)-3-benzyl-*sn*-glycerol was deprotected to give **1B** in 50% yield. [α]_D²⁰ = -14.8 (*c* 0.18, CHCl₃); IR (neat) 3449 (OH), 2960 (CH), 1719 (C=O), 1654 (C=C), cm⁻¹; ¹H NMR (250 MHz, CDCl₃) δ 1.03 (2 d, *J* = 6.6 Hz, 6 H, C(O)CH₂CHMe₂), 1.99 (d, *J* = 1.2 Hz, 3 H, C(O)CH=CMe₂), 2.10–2.35 (m, 3 H, C(O)CH₂CHMe₂ containing 2.25 (d, *J* = 1.2 Hz, 3 H, C(O)CH=CMe₂), 3.81 (br s, 2 H, HOCH₂CH(O-)CH₂O), 4.37 (2 overlapping AB quartets, 2 H, HOCH₂CH(O-)CH₂O), 5.14–5.22 (m, 1 H, HOCH₂CH(O-)CH₂O), 5.75–5.79 (m, 1 H, -C(O)CH=CMe₂); ¹³C NMR (62.5 MHz, CDCl₃) δ 20.29, 22.29, 25.58, 27.41, 43.10, 61.64, 61.99, 71.35, 115.25, 158.33, 165.77, 172.87; FAB-MS (*m/z*, relative intensity): 259 (MH⁺, 27), 83 (100). Anal. (C₁₃H₂₂O₅) C, H.

1-(3-Methylbutanoyl)-2-(3-isopropyl-4-methylpentanoyl)-*sn*-glycerol (1C). Palladium on carbon (100 mg, 10%) was added to a suspension of the intermediate 1-(3-methylbutanoyl)-2-(3-isopropyl-4-methylpentanoyl)-3-benzyl-*sn*-glycerol (525 mg) in methanol (20 mL), and the mixture was stirred under H₂ (45 psi) overnight. The crude reaction mixture was filtered, and the filtrate was concentrated under reduced pressure. Purification by silica gel chromatography (gradient elution from 5% EtOAc/hexane to 50% EtOAc/hexane) gave **1C** (0.15 g, 0.46 mmol, 45%). [α]_D²⁰ = -2.44 (*c* 1.27, CHCl₃); IR (neat) 3463 (OH), 2960 (CH), 2875 (CH), 1740 (C=O) cm⁻¹; ¹H NMR (250 MHz, CDCl₃) δ 0.90 and 0.99 (d, *J* = 6.6 Hz, 12 H, C(O)CH₂CH(CHMe₂)₂), 1.04 (d, *J* = 6.3 Hz, 6 H, C(O)CH₂CH(CHMe₂)₂), 1.70 (pentet, *J* = 5.8 Hz, 1 H, C(O)CH₂CH(CHMe₂)₂), 1.83 (heptet, *J* = 6.5 Hz, 2 H, C(O)CH₂CH(CHMe₂)₂), 2.08–2.33 (m, 5 H, C(O)CH₂CHMe₂ and C(O)CH₂CH(CHMe₂)₂), 3.81 (d, *J* = 4.9 Hz, 2 H, HOCH₂CH(O-)CH₂O), 4.32 (dd, *J* = 12.0, 5.7 Hz, 1 H, HOCH₂CH(O-)CH₂O), 4.41 (dd, *J* = 12.0, 4.4 Hz, 1 H, HOCH₂CH(O-)CH₂O), 5.05–5.20 (m, 1 H, HOCH₂CH(O-)CH₂O); ¹³C NMR (62.5 MHz, CDCl₃) δ 18.63, 18.68, 21.26, 21.28, 22.28, 25.54, 29.28, 29.35, 32.92, 43.05, 46.71, 61.30, 61.99, 72.08, 172.84, 174.34; FAB-MS (*m/z*, relative intensity): 317 (MH⁺, 16), 57 (100). Anal. (C₁₇H₃₂O₅) C, H.

1-(3-Methylbutanoyl)-2-(3-isopropyl-4-methylpent-2-enoyl)-*sn*-glycerol (1D). According to the general procedure,

1-(3-methylbutanoyl)-2-(3-isopropyl-4-methylpent-2-enoyl)-3-benzyl-*sn*-glycerol was deprotected to give **1D** in 44% yield. $[\alpha]^{20}_D = -4.6$ (c 1.36, CHCl₃); IR (neat) 3478 (OH), 2963 (CH), 2873 (CH), 1722 (C=O), 1634 (C=C) cm⁻¹; ¹H NMR (250 MHz, CDCl₃) δ 1.02 (d, $J = 6.6$ Hz, 6 H, C(O)CH₂CHMe₂), 1.13 and 1.14 (d, $J = 6.8$ Hz, 12 H, C(O)CH=CH(CHMe₂)₂), 2.16 (heptet, $J = 6.6$ Hz, 1 H, C(O)CH₂CHMe₂), 2.28 (d, $J = 6.6$ Hz, 2 H, C(O)CH₂CHMe₂), 2.44 (br t, $J = 7.3$ Hz, 1 H, HOCH₂CH(O-)CH₂O), 2.64 (heptet, $J = 6.8$ Hz, 1 H, C(O)CH=CH(CHMe₂)₂), 3.83 (t, $J = 5.4$ Hz, 2 H, HOCH₂CH(O-)CH₂O), 4.10 (heptet, $J = 6.8$ Hz, 1 H, C(O)CH=CH(CHMe₂)₂), 4.37 (2 overlapping doublets, $J = 5.3, 4.9$ Hz, 2 H, HOCH₂CH(O-)CH₂O), 5.10–5.25 (m, 1 H, HOCH₂CH(O-)CH₂O), 5.73 (s, 1 H, C(O)CH=CH(CHMe₂)₂); ¹³C NMR (62.5 MHz, CDCl₃) δ 20.13, 20.20, 22.29, 24.07, 25.59, 29.05, 29.79, 43.11, 61.61, 62.01, 71.31, 111.93, 166.18, 172.87, 177.82; FAB-MS (m/z , relative intensity): 315 (MH⁺, 31), 139 (100). Anal. (C₁₇H₃₀O₅) C, H.

1-(3-Methylbut-2-enoyl)-2-(3-methylbutanoyl)-*sn*-glycerol (2A). According to the general procedure, 1-(3-methylbut-2-enoyl)-2-(3-methylbutanoyl)-3-benzyl-*sn*-glycerol was deprotected to give **2A** in 67% yield. $[\alpha]^{20}_D = -11.2$ (c 0.92, CHCl₃); IR (neat) 3478 (OH), 2960 (CH), 2873 (CH), 1722 (C=O), 1651 (C=C) cm⁻¹; ¹H NMR (250 MHz, CDCl₃) δ 1.02 (d, $J = 6.6$ Hz, 6 H, C(O)CH₂CHMe₂), 1.97 (s, 3 H, C(O)CH=CHMe₂), 2.11–2.31 (m, 3 H, C(O)CH₂CHMe₂ containing 2.23 (d, $J = 1.0$ Hz, 3 H, C(O)CH=CHMe₂), 2.55 (br s, 1 H, HOCH₂CH(O-)CH₂O), 3.79 (d, $J = 4.9$ Hz, 2 H, HOCH₂CH(O-)CH₂O), 4.36 (2 overlapping AB quartets, 2 H, HOCH₂CH(O-)CH₂O), 5.13–5.21 (m, 1 H, HOCH₂CH(O-)CH₂O), 5.75 (m, 1 H, C(O)CH=CHMe₂); ¹³C NMR (62.5 MHz, CDCl₃) δ 20.27, 22.23, 25.67, 27.39, 43.08, 61.22, 61.33, 72.10, 115.10, 158.08, 166.24, 172.54; FAB-MS (m/z , relative intensity): 259 (MH⁺, 29), 83 (100). Anal. (C₁₃H₂₂O₅) C, H.

1,2-Di-(3-methylbut-2-enoyl)-*sn*-glycerol (2B). According to the general procedure, 1,2-di-(3-methylbut-2-enoyl)-3-benzyl-*sn*-glycerol was deprotected to give **2B** in 92% yield. $[\alpha]^{20}_D = -27.07$ (c 3.65, CHCl₃); IR (neat) 3481 (OH), 2941 (CH), 1716 (C=O), 1652 (C=C) cm⁻¹; ¹H NMR (250 MHz, CDCl₃) δ 1.98 and 2.24 (s, 12 H, C(O)CH=CHMe₂), 2.48 (br s, 1 H, HOCH₂CH(O-)CH₂O), 3.81 (d, $J = 4.9$ Hz, 2 H, HOCH₂CH(O-)CH₂O), 4.38 (d, $J = 5.1$ Hz, 2 H, HOCH₂CH(O-)CH₂O), 5.13–5.21 (m, 1 H, HOCH₂CH(O-)CH₂O), 5.77 and 5.79 (br s, 2 H, C(O)CH=CHMe₂); ¹³C NMR (62.5 MHz, CDCl₃) δ 20.24, 27.36, 61.37, 61.40, 71.46, 115.22, 115.39, 157.83, 158.02, 165.80, 166.28. FAB-MS (m/z , relative intensity): 257 (MH⁺, 31), 83 (100). Anal. (C₁₃H₂₀O₅) C, H.

1-(3-Methylbut-2-enoyl)-2-(3-isopropyl-4-methylpentanoyl)-*sn*-glycerol (2C). According to the general procedure, 1-(3-methylbut-2-enoyl)-2-(3-isopropyl-4-methylpentanoyl)-3-benzyl-*sn*-glycerol was deprotected to give **2C** in quantitative yield. $[\alpha]^{20}_D = -11.16$ (c 0.65, CHCl₃); IR (neat) 3487 (OH), 2960 (CH), 1724 (C=O), 1654 (C=C) cm⁻¹; ¹H NMR (250 MHz, CDCl₃) δ 0.90 and 0.99 (d, $J = 6.6$ Hz, 12 H, C(O)CH₂CH(CHMe₂)₂), 1.71 (pentet, $J = 5.7$ Hz, 1 H, C(O)CH₂CH(CHMe₂)₂), 1.82 (heptet, $J = 6.3$ Hz, 2 H, C(O)CH₂CH(CHMe₂)₂), 1.99 (d, $J = 0.74$ Hz, 3 H, C(O)CH=CHMe₂), 2.25 (d, $J = 1.0$ Hz, 3 H, C(O)CH=CHMe₂), 2.31 (d, $J = 5.6$ Hz, 2 H, C(O)CH₂CH(CHMe₂)₂), 3.81 (d, $J = 4.9$ Hz, 2 H, HOCH₂CH(O-)CH₂O), 4.38 (d, $J = 5.1$ Hz, 2 H, HOCH₂CH(O-)CH₂O), 5.13–5.21 (m, 1 H, HOCH₂CH(O-)CH₂O), 5.76 (t, $J = 1.2$ Hz, 1 H, C(O)CH=CHMe₂); ¹³C NMR (62.5 MHz, CDCl₃) δ 18.67, 18.70, 20.29, 21.29, 27.41, 29.31, 29.36, 32.96, 46.74, 61.12, 61.37, 72.24, 115.11, 158.13, 166.27, 174.35. FAB-MS (m/z , relative intensity): 315 (MH⁺, 19), 83 (100). Anal. (C₁₇H₃₀O₅) C, H.

1-(3-Methylbut-2-enoyl)-2-(3-isopropyl-4-methylpent-2-enoyl)-*sn*-glycerol (2D). According to the general procedure, 1-(3-methylbut-2-enoyl)-2-(3-isopropyl-4-methylpent-2-enoyl)-3-benzyl-*sn*-glycerol was deprotected to give **2D** in 95% yield. $[\alpha]^{20}_D = -26.53$ (c 0.48, CHCl₃); IR (neat) 3482 (CO), 2965 (CH), 2872 (CH), 1719 (C=O), 1638 (C=C), cm⁻¹; ¹H NMR (250 MHz, CDCl₃) δ 1.09–1.14 (m, 12 H, C(O)CH=CH(CHMe₂)₂), 1.96 and 2.23 (d, $J = 1.0$ Hz, 6 H, C(O)CH=CHMe₂), 2.50–2.55 (m, 2 H, C(O)CH=CH(CHMe₂)₂ and HOCH₂CH(O-)CH₂O),

3.79–3.81 (m, 2 H, HOCH₂CH(O-)CH₂O), 4.07 (heptet, $J = 6.8$ Hz, 1 H, C(O)CH=CH(CHMe₂)₂), 4.36 (d, $J = 5.1$ Hz, 2 H, HOCH₂CH(O-)CH₂O), 5.13–5.20 (m, 1 H, HOCH₂CH(O-)CH₂O), 5.71 (s, 1 H, C(O)CH=CH(CHMe₂)₂), 5.79 (t, $J = 1.2$ Hz, 1 H, C(O)CH=CHMe₂); ¹³C NMR (62.5 MHz, CDCl₃) δ 20.17, 20.27, 24.08, 27.40, 28.97, 29.77, 61.40, 61.47, 71.53, 111.89, 115.38, 158.13, 165.82, 166.76, 177.36; FAB-MS (m/z , relative intensity): 313 (MH⁺, 40), 139 (97), 83 (100). Anal. (C₁₇H₂₈O₅) C, H.

1-(3-Isopropyl-4-methylpentanoyl)-2-(3-methylbutanoyl)-*sn*-glycerol (3A). According to the general procedure, 1-(3-isopropyl-4-methylpentanoyl)-2-(3-methylbutanoyl)-3-benzyl-*sn*-glycerol was deprotected to give **3A** in 77% yield. $[\alpha]^{20}_D = -3.80$ (c 2.12, CDCl₃); IR (neat) 3468 (OH), 2960 (CH), 2874 (CH), 1741 (C=O) cm⁻¹; ¹H NMR (250 MHz, CDCl₃) δ 0.86 (d, $J = 6.6$ Hz, 6 H, C(O)CH₂CH(CHMe₂)₂), 0.95 (d, $J = 6.8$ Hz, 6 H, C(O)CH₂CHMe₂), 1.02 (d, $J = 6.6$ Hz, 6 H, C(O)CH₂CH(CHMe₂)₂), 1.65 (pentet, $J = 5.8$ Hz, 1 H, C(O)CH₂CH(CHMe₂)₂), 1.80 (heptet, $J = 6.5$ Hz, 2 H, C(O)CH₂CH(CHMe₂)₂), 2.10–2.29 (m, 5 H, C(O)CH₂CH(CHMe₂)₂ and -C(O)CH₂CHMe₂), 2.54 (br s, 1 H, HOCH₂CH(O-)CH₂O), 3.78 (d, $J = 5.1$ Hz, 2 H, HOCH₂CH(O-)CH₂O), 4.25 (dd, $J = 12.0, 5.9$ Hz, 1 H, HOCH₂CH(O-)CH₂O), 4.38 (dd, $J = 12.0, 4.2$ Hz, 1 H, HOCH₂CH(O-)CH₂O), 5.11–5.19 (m, 1 H, HOCH₂CH(O-)CH₂O); ¹³C NMR (62.5 MHz, CDCl₃) δ 18.63, 21.24, 22.24, 25.64, 29.27, 32.72, 43.24, 46.68, 61.35, 62.23, 71.99, 172.54, 174.64. FAB-MS (m/z , relative intensity): 317 (MH⁺, 32), 159 (100), 57 (100). Anal. (C₁₇H₃₂O₅) C, H.

1-(3-Isopropyl-4-methylpentanoyl)-2-(3-methylbut-2-enoyl)-*sn*-glycerol (3B). According to the general procedure, 1-(3-isopropyl-4-methylpentanoyl)-2-(3-methylbut-2-enoyl)-3-benzyl-*sn*-glycerol was deprotected to give **3B** in 94% yield. $[\alpha]^{20}_D = -10.24$ (c 1.69, CDCl₃); IR (neat) 3467 (OH), 2960 (CH), 1723 (C=O), 1653 (C=C) cm⁻¹; ¹H NMR (250 MHz, CDCl₃) δ 0.89 (d, $J = 6.8$ Hz, 6 H, C(O)CH₂CH(CHMe₂)₂), 0.98 (d, $J = 6.6$ Hz, 6 H, C(O)CH₂CH(CHMe₂)₂), 1.69 (pentet, $J = 5.7$ Hz, 1 H, C(O)CH₂CH(CHMe₂)₂), 1.75–1.95 (m, 2 H, C(O)CH₂CH(CHMe₂)₂), 1.99 and 2.26 (d, $J = 0.74$ Hz, 6 H, C(O)CH=CHMe₂), 2.28 (d, $J = 5.6$ Hz, 2 H, C(O)CH₂CH(CHMe₂)₂), 3.84 (d, $J = 4.9$ Hz, 2 H, HOCH₂CH(O-)CH₂O), 4.36 (2 overlapping AB quartets, 2 H, HOCH₂CH(O-)CH₂O), 5.15–5.23 (m, 1 H, HOCH₂CH(O-)CH₂O), 5.79 (s, 1 H, C(O)CH=CHMe₂); ¹³C NMR (62.5 MHz, CDCl₃) δ 18.66, 20.29, 21.25, 27.41, 29.29, 32.77, 46.70, 61.66, 62.23, 71.39, 115.29, 158.27, 165.80, 174.66. FAB-MS (m/z , relative intensity): 315 (MH⁺, 18), 83 (100). Anal. (C₁₇H₃₀O₅·0.2H₂O) C, H.

1,2-Di-(3-isopropyl-4-methylpentanoyl)-*sn*-glycerol (3C). This compound was prepared as previously reported in ref 16.

1-(3-Isopropyl-4-methylpentanoyl)-2-(3-isopropyl-4-methylpent-2-enoyl)-*sn*-glycerol (3D). According to the general procedure, 1-(3-isopropyl-4-methylpentanoyl)-2-(3-isopropyl-4-methylpent-2-enoyl)-3-benzyl-*sn*-glycerol was deprotected to give **3D** in 90% yield. $[\alpha]^{20}_D = -4.97$ (c = 0.93, CDCl₃); IR (neat) 3482 (OH), 2960 (CH), 2879 (CH), 1718 (C=O), 1637 (C=C) cm⁻¹; ¹H NMR (250 MHz, CDCl₃) δ 0.88 (d, $J = 6.8$ Hz, 6 H, C(O)CH₂CH(CHMe₂)₂), 0.96 (d, $J = 6.6$ Hz, 6 H, C(O)CH₂CH(CHMe₂)₂), 1.13 and 1.14 (d, $J = 6.8$ Hz, 12 H, CH=CH(CHMe₂)₂), 1.20–1.80 (m, 3 H, C(O)CH₂CH(CHMe₂)₂), 2.27 (d, $J = 5.6$ Hz, 2 H, C(O)CH₂CH(CHMe₂)₂), 2.42 (br s, 1 H, HOCH₂CH(O-)CH₂O), 2.63 (heptet, $J = 7.1$ Hz, 1 H, C(O)CH=CH(CHMe₂)₂), 3.83 (d, $J = 4.9$ Hz, 2 H, HOCH₂CH(O-)CH₂O), 4.11 (heptet, $J = 7.1$ Hz, 1 H, C(O)CH=CH(CHMe₂)₂), 4.36 (2 overlapping AB quartets, 2 H, HOCH₂CH(O-)CH₂O), 5.12–5.21 (m, 1 H, HOCH₂CH(O-)CH₂O), 5.73 (s, 1 H, C(O)CH=CH(CHMe₂)₂); ¹³C NMR (62.5 MHz, CDCl₃) δ 18.64, 18.68, 20.15, 20.20, 21.29, 24.07, 29.05, 29.29, 29.33, 29.78, 32.78, 46.73, 61.68, 62.22, 71.37, 111.95, 166.18, 174.65, 177.80; FAB-MS (m/z , relative intensity): 371 (MH⁺, 17), 139 (100). Anal. (C₂₁H₃₈O₅) C, H.

1-(3-Isopropyl-4-methylpent-2-enoyl)-2-(3-methylbutanoyl)-*sn*-glycerol (4A). According to the general procedure, 1-(3-isopropyl-4-methylpent-2-enoyl)-2-(3-methylbutanoyl)-3-benzyl-*sn*-glycerol was deprotected to give **4A** in 89% yield.

$[\alpha]_D^{20} = -46.3$ (c 0.58, CHCl_3); IR (neat) 3478 (OH), 2964 (CH), 2873 (CH), 1722 (C=O), 1634 (C=C) cm^{-1} ; ^1H NMR (250 MHz, CDCl_3) δ 1.02 (d, $J = 6.6$ Hz, 6 H, $\text{C}(\text{O})\text{CH}_2\text{CHMe}_2$), 1.11 (d, $J = 6.8$ Hz, 6 H, $\text{C}(\text{O})\text{CH}=\text{C}(\text{CHMe}_2)_2$), 1.13 (d, $J = 6.6$ Hz, 6 H, $\text{C}(\text{O})\text{CH}=\text{C}(\text{CHMe}_2)_2$), 2.17 (heptet, $J = 6.6$ Hz, 1 H, $\text{C}(\text{O})\text{CH}_2\text{CHMe}_2$), 2.30 (d, $J = 6.6$ Hz, 2 H, $\text{C}(\text{O})\text{CH}_2\text{CHMe}_2$), 2.62 (heptet, $J = 6.8$ Hz, 1 H, $\text{C}(\text{O})\text{CH}=\text{C}(\text{CHMe}_2)_2$), 3.79 (d, $J = 4.2$ Hz, 2 H, $\text{HOCH}_2\text{CH}(\text{O}-)\text{CH}_2\text{O}$), 4.08 (heptet, $J = 6.9$ Hz, 1 H, $\text{C}(\text{O})\text{CH}=\text{C}(\text{CHMe}_2)_2$), 4.34 (2 overlapping AB quartets, 2 H, $\text{HOCH}_2\text{CH}(\text{O}-)\text{CH}_2\text{O}$), 5.14–5.23 (m, 1 H, $\text{HOCH}_2\text{CH}(\text{O}-)\text{CH}_2\text{O}$), 5.70 (s, 1 H, $\text{C}(\text{O})\text{CH}=\text{C}(\text{CHMe}_2)_2$); ^{13}C NMR (62.5 MHz, CDCl_3) δ 20.17, 22.24, 24.06, 25.68, 28.98, 29.76, 43.28, 61.27, 61.36, 72.12, 111.79, 166.64, 172.56, 177.53. FAB-MS (m/z , relative intensity): 315 (MH^+ , 33), 139 (100). Anal. ($\text{C}_{17}\text{H}_{30}\text{O}_5 \cdot 0.4\text{H}_2\text{O}$) C, H.

1-(3-Isopropyl-4-methylpent-2-enoyl)-2-(3-methylbut-2-enoyl)-sn-glycerol (4B). According to the general procedure, 1-(3-isopropyl-4-methylpent-2-enoyl)-2-(3-methylbut-2-enoyl)-3-benzyl-sn-glycerol was deprotected to give **4B** in 81% yield. $[\alpha]_D^{20} = -46.26$ (c 5.8, CHCl_3); IR (neat) 3492 (OH), 2966 (CH), 2873 (CH), 1722 (C=O), 1651 (C=C) cm^{-1} ; ^1H NMR (250 MHz, CDCl_3) δ 1.13 (t, $J = 6.3$ Hz, 12 H, $\text{C}(\text{O})\text{CH}=\text{C}(\text{CHMe}_2)_2$), 1.97 and 2.24 (d, $J = 0.7$ Hz, 6 H, $\text{C}(\text{O})\text{CH}=\text{CMe}_2$), 2.52 (br s, 1 H, $\text{HOCH}_2\text{CH}(\text{O}-)\text{CH}_2\text{O}$), 2.63 (heptet, $J = 6.8$ Hz, 1 H, $\text{C}(\text{O})\text{CH}=\text{C}(\text{CHMe}_2)_2$), 3.82 (d, $J = 4.9$ Hz, 2 H, $\text{HOCH}_2\text{CH}(\text{O}-)\text{CH}_2\text{O}$), 4.08 (heptet, $J = 6.8$ Hz, 1 H, $\text{C}(\text{O})\text{CH}=\text{C}(\text{CHMe}_2)_2$), 4.37 (d, $J = 5.1$ Hz, 2 H, $\text{HOCH}_2\text{CH}(\text{O}-)\text{CH}_2\text{O}$), 5.13–5.21 (m, 1 H, $\text{HOCH}_2\text{CH}(\text{O}-)\text{CH}_2\text{O}$), 5.72 (s, 1 H, $\text{C}(\text{O})\text{CH}=\text{C}(\text{CHMe}_2)_2$), 5.80 (br s, 1H, $-\text{C}(\text{O})\text{CH}=\text{CMe}_2$); ^{13}C NMR (62.5 MHz, CDCl_3) δ 20.17, 20.28, 24.08, 27.40, 28.99, 29.79, 61.37, 61.52, 71.55, 111.89, 115.37, 158.13, 165.82, 166.76, 177.38. FAB-MS (m/z , relative intensity): 313 (MH^+ , 23), 139 (100). Anal. ($\text{C}_{17}\text{H}_{28}\text{O}_5$) C, H.

1-(3-Isopropyl-4-methylpent-2-enoyl)-2-(3-isopropyl-4-methylpentanoyl)-sn-glycerol (4C). According to the general procedure, 1-(3-isopropyl-4-methylpent-2-enoyl)-2-(3-isopropyl-4-methylpentanoyl)-3-benzyl-sn-glycerol was deprotected to give **4C** in 86% yield. $[\alpha]_D^{20} = -10.04$ (c 0.44 CHCl_3); IR (neat) 3475 (OH), 2962 (CH), 2873 (CH), 1720 (C=O), 1637 (C=C) cm^{-1} ; ^1H NMR (250 MHz, CDCl_3) δ 0.90 and 0.99 (d, $J = 6.6$ Hz, 12 H, $\text{C}(\text{O})\text{CH}_2\text{CH}(\text{CHMe}_2)_2$), 1.13 (d, $J = 6.8$ Hz, 6 H, $\text{C}(\text{O})\text{CH}=\text{C}(\text{CHMe}_2)_2$), 1.15 (d, $J = 6.6$ Hz, 6 H, $\text{C}(\text{O})\text{CH}=\text{C}(\text{CHMe}_2)_2$), 1.65–1.91 (m, 3 H, $\text{C}(\text{O})\text{CH}_2\text{CH}(\text{CHMe}_2)_2$), 2.27 (d, $J = 5.6$ Hz, 2 H, $\text{C}(\text{O})\text{CH}_2\text{CH}(\text{CHMe}_2)_2$), 2.64 (heptet, $J = 6.8$ Hz, 1 H, $\text{C}(\text{O})\text{CH}=\text{C}(\text{CHMe}_2)_2$), 3.82 (d, $J = 4.9$ Hz, 2 H, $\text{HOCH}_2\text{CH}(\text{O}-)\text{CH}_2\text{O}$), 4.11 (heptet, $J = 6.8$ Hz, 1 H, $\text{C}(\text{O})\text{CH}=\text{C}(\text{CHMe}_2)_2$), 4.33–4.41 (m, 2 H, $\text{HOCH}_2\text{CH}(\text{O}-)\text{CH}_2\text{O}$), 5.13–5.21 (m, 1 H, $\text{HOCH}_2\text{CH}(\text{O}-)\text{CH}_2\text{O}$), 5.72 (s, 1H, $\text{C}(\text{O})\text{CH}=\text{C}(\text{CHMe}_2)_2$); ^{13}C NMR (62.5 MHz, CDCl_3) δ 18.66, 18.72, 20.20, 21.31, 24.09, 29.02, 29.32, 29.38, 29.79, 32.97, 46.76, 61.17, 61.44, 72.29, 111.78, 166.68, 174.39, 177.64; FAB-MS (m/z , relative intensity): 371 (MH^+ , 10), 139 (100). Anal. ($\text{C}_{21}\text{H}_{38}\text{O}_5$) C, H.

1,2-Di-(3-isopropyl-4-methylpent-2-enoyl)-sn-glycerol (4D). According to the general procedure, 1,2-di-(3-isopropyl-4-methylpent-2-enoyl)-3-benzyl-sn-glycerol was deprotected to give **4D** in 99% yield. $[\alpha]_D^{20} = -15.58$ (c 1.54, CHCl_3); IR (neat) 3474 (OH), 2965 (CH), 2875 (CH), 1717 (C=O), 1637 (C=C) cm^{-1} ; ^1H NMR (250 MHz, CDCl_3) δ 1.12–1.18 (m, 24 H, $\text{C}(\text{O})\text{CH}=\text{C}(\text{CHMe}_2)_2$), 2.31 (br s, 1 H, $\text{HOCH}_2\text{CHCH}_2\text{O}$), 2.64 (heptet, $J = 6.8$ Hz, 1 H, $\text{C}(\text{O})\text{CH}=\text{C}(\text{CHMe}_2)_2$), 2.65 (heptet, $J = 6.8$ Hz, 1 H, $\text{C}(\text{O})\text{CH}=\text{C}(\text{CHMe}_2)_2$), 3.85 (d, $J = 4.9$ Hz, 2 H, $\text{HOCH}_2\text{CH}(\text{O}-)\text{CH}_2\text{O}$), 4.10 (heptet, $J = 6.8$ Hz, 1 H, $\text{C}(\text{O})\text{CH}=\text{C}(\text{CHMe}_2)_2$), 4.12 (heptet, $J = 6.8$ Hz, 1 H, $\text{C}(\text{O})\text{CH}=\text{C}(\text{CHMe}_2)_2$), 4.39 (d, $J = 5.1$ Hz, 2 H, $\text{HOCH}_2\text{CH}(\text{O}-)\text{CH}_2\text{O}$), 5.13–5.21 (m, 1 H, $\text{HOCH}_2\text{CH}(\text{O}-)\text{CH}_2\text{O}$), 5.75 and 5.77 (s, 1 H, $\text{C}(\text{O})\text{CH}=\text{C}(\text{CHMe}_2)_2$); ^{13}C NMR (62.5 MHz, CDCl_3) δ 20.16, 20.20, 24.07, 29.01, 29.07, 29.80, 61.35, 61.54, 71.57, 111.91, 112.07, 166.22, 166.76, 177.35, 177.56; FAB-MS (m/z , relative intensity): 369 (MH^+ , 14), 139 (100). Anal. ($\text{C}_{21}\text{H}_{36}\text{O}_5$) C, H.

Acknowledgment. Zinc finger geometries of PK-C were kindly provided by Dr. Igor A. Topol of the

Advanced Biomedical Computing Center, National Cancer Institute at Frederick, National Institutes of Health, Frederick, MD. Some of the computational studies were performed on the SGI Origin 2000 system at the Center for Information Technology, National Institutes of Health, Bethesda, MD.

References

- (1) Newton, A. C. Protein Kinase C: Structure, function and regulation. *J. Biol. Chem.* **1995**, *270*, 28495–28498.
- (2) Quest, A. F. G. Regulation of protein kinase C: A tale of lipids and proteins. *Enzyme Protein* **1996**, *49*, 231–261.
- (3) Mellor, H.; Parker, P. J. The extended protein kinase C superfamily. *Biochem. J.* **1998**, *332*, 281–292.
- (4) Ron, D.; Kazanietz, M. G. New insights into the regulation of protein kinase C and novel phorbol ester receptors. *FASEB J.* **2000**, *13*, 1658–1676.
- (5) Sakai, N.; Sadaki, K.; Ikegaki, N.; Shirai, Y.; Ono, Y.; Saito, N. Direct visualization of the translocation of the γ -subspecies of protein kinase C in living cells using fusion proteins with green fluorescent protein. *J. Cell Biol.* **1997**, *139*, 1465–1476.
- (6) Oancea, E.; Teruel, M. N.; Quest, A. F. G.; Meyer, T. Green fluorescent protein (GFP)-tagged cysteine-rich domains from protein kinase C as fluorescent indicators for diacylglycerol signaling in living cells. *J. Cell Biol.* **1998**, *140*, 485–498.
- (7) Newton, A. C.; Keranen, L. M. Phosphatidyl-L-serine is necessary for protein kinase C's high affinity interaction with diacylglycerol-containing membranes. *Biochemistry* **1994**, *33*, 661–6658.
- (8) Newton, A. C. Regulation of protein kinase C. *Curr. Opin. Cell Biol.* **1997**, *9*, 161–167.
- (9) Nishizuka, Y. Intracellular signaling by hydrolysis of phospholipids and activation of protein-kinase-C. *Science* **1992**, *258*, 607–614.
- (10) Oancea, E.; Meyer, T. Protein kinase C as a molecular machine for decoding calcium and diacylglycerol signals. *Cell* **1998**, *95*, 307–318.
- (11) Fishman, D. D.; Segal, S.; Livneh, E. The role of protein kinase C in G1 and G2/M phases of the cell cycle. *Int. J. Oncol.* **1998**, *12*, 181–186.
- (12) Zhang, G. G.; Kazanietz, M. G.; Blumberg, P. M.; Hurley, J. H. Crystal structure of the cys2 activator-binding domain of protein kinase C delta in complex with phorbol ester. *Cell* **1995**, *81*, 917–914.
- (13) Sharkey, N. A.; Leach, K. L.; Blumberg, P. M. Competitive inhibition by diacylglycerol of specific phorbol ester binding. *Proc. Natl. Acad. Sci. U.S.A.* **1984**, *81*, 607–610.
- (14) Marquez, V. E.; Nacro, K.; Benzaria, S.; Lee, J.; Sharma, R.; Teng, K.; Milne, G. W. A.; Bienfait, B.; Wang, S.; Lewin, N. E.; Blumberg, P. M. The transition from a pharmacophore-guided approach to a receptor-guided approach in the design of potent kinase C ligands. *Pharmacol. Therap.* **1999**, *82*, 251–261.
- (15) Nacro, K.; Bienfait, B.; Lee, J.; Han, K.-C.; Kang, J.-H.; Benzaria, S.; Lewin, N. E.; Bhattacharyya, D. K.; Blumberg, P. M.; Marquez, V. E. Conformationally constrained analogues of diacylglycerol (DAG). 16. How much structural complexity is necessary for recognition and high binding affinity to protein kinase C? *J. Med. Chem.* **2000**, *43*, 921–944.
- (16) Nacro, K.; Bienfait, B.; Lewin, N. E.; Blumberg, P. M.; Marquez, V. E. Diacylglycerols with lipophilically equivalent branched acyl chains display high affinity for protein kinase C (PK-C). A direct measure of the effect of constraining the glycerol backbone in DAG lactones. *Bioorg. Med. Chem. Lett.* **2000**, *10*, 653–655.
- (17) Meylan, W. M.; Howard, Ph. H. *KOWWIN 1.63*, Syracuse Research Corp.; <http://esc.syrres.com.20>. *J. Pharm. Sci.* **1995**, *84*, 83.
- (18) Wang, Q. M. J.; Bhattacharyya, D.; Garfield, S.; Nacro, K.; Marquez, V. E.; Blumberg, P. M. Differential localization of protein kinase C delta by phorbol esters and related compounds using a fusion protein with green fluorescent protein. *J. Biol. Chem.* **1999**, *274*, 37233–37239.
- (19) Morris, G. M.; Goodsell, D. S.; Huey, R.; Olson, A. J. Distributed automatic docking of flexible ligands to proteins: Parallel applications of autodock 2.4. *J. Comput.-Aid. Mol. Des.* **1996**, *10*, 293–304.
- (20) Schrödinger, Inc., Portland, OR. <http://www.schrodinger.com>
- (21) Molecular Simulations Inc., San Diego, CA. <http://www.msi.com>
- (22) Brooks, B. R.; Brucoleri, R. E.; Olafson, B. D.; States, D. J.; Swaminathan, S.; Karplus, M. CHARMM: A program for macromolecular energy minimization and dynamics calculations. *J. Comput. Chem.* **1983**, *4*, 187–217.

- (23) MacKerell, A. D., Jr.; Bashford, D.; Bellott, M.; Dunbrack, R. L., Jr.; Evanseck, J. D.; Field, M. J.; Fischer, S.; Gao, J.; Guo, H.; Ha, S.; Joseph-McCarthy, D.; Kuchnir, L.; Kucsera, K.; Lau, F. T. K.; Mattos, C.; Michnick, S.; Ngo, T.; Nguyen, D. T.; Prodhom, B.; Reiher, III, W. E.; Roux, B.; Schlenkrich, M.; Smith, J. C.; Stote, R.; Straub, J.; Watanabe, M.; Wiorkiewicz-Kuczera, J.; Yin, D.; Karplus, M. All-atom empirical potential for molecular modeling and dynamics studies of proteins. *J. Phys. Chem. B* **1998**, *102*, 3586–3616.
- (24) Topol, A. I.; Nemukhim, A. V.; Chao, M.; Iyer, L. K.; Tawa, G. J.; Burt, S. K. Quantum chemical studies of reactions of the cyclic disulfides with the zinc finger domains in the HIV-1 nucleocapsid protein (NCp7). *J. Am. Chem. Soc.* **2000**, *122*, 7087–7094.
- (25) Kazanietz, M. G.; Areces, L. B.; Bahador, A.; Mischak, H.; Goodnight, J.; Mushinski, J. F.; Blumberg, P. M. Characterization of ligand and substrate specificity for the calcium-dependent and calcium-independent protein kinase-C isozymes. *Mol. Pharmacol.* **1993**, *44*, 298–307.
- (26) Lorenzo, P. S.; Bogi, K.; Hughes, K. M.; Beheshti, M.; Garfield, S. H.; Pettit, G. R.; Blumberg, P. M. Differential roles of the tandem C-1 domains of PKC- δ in the biphasic down-regulation induced by bryostatin 1. *Cancer Res.* **1999**, *59*, 6137–6144.

JM010052E